International Journal of Heat and Mass Transfer 179 (2021) 121723

Contents lists available at ScienceDirect

International Journal of Heat and Mass Transfer

journal homepage: www.elsevier.com/locate/hmt

Review

Boiling process assessment for absorption heat pumps: A review

Carlos Amaris [a], Mahmoud Bourouis [b,*]

[a] Universidad de la Costa, Department of Energy, Cl. 58 #55-66, 080002 Barranquilla, Colombia
[b] Universitat Rovira i Virgili, Department of Mechanical Engineering, Av. Països Catalans No. 26, 43007 Tarragona, Spain

ARTICLE INFO

Article history:
Received 21 May 2021
Revised 4 July 2021
Accepted 10 July 2021

Keywords:
Absorption heat pumps
Desorber
Boiling process
Nucleate boiling
Convective boiling
Boiling heat transfer correlations

ABSTRACT

Absorption technology becomes an attractive option for cooling or heating when driven by solar thermal energy, residual heat from different processes, or geothermal energy. Further development of this technology could help to cover current cooling or heating requirements and have a much lower impact on the environment than mechanical compression cooling and heat pumps systems. Moreover, the rising cost of electrical energy added to the issue of climate change are reasons to move towards the development of environmental and sustainable energy technologies. The desorbers are key components of absorption heat pump technologies. Studies in the open literature on desorbers show advances in new design concepts to enhance heat and mass transfer with different working fluids. Therefore, the objective of this review is to identify, summarise, and discuss the experimental studies that deal with the boiling process in desorbers and boiling correlations specifically for use in absorption heat pump technologies. It includes a comprehensive scrutiny on the boiling phenomenon in pool desorbers, falling-film desorbers, and forced flow desorbers for conventional and promising working fluids, and details the experimental techniques and the latest advances in desorber design concepts. Finally, the review contains proposals for future studies to be carried out so as to contribute to the further development of absorption heat pump technologies.

1. Introduction

Absorption technology becomes an attractive option for cooling or heating when driven by solar thermal energy [1–4], residual heat from different processes [5–9], or geothermal energy [10]. The further evolution of this technology would facilitate its diffusion around the world, help to cover current cooling or heating requirements and have a much lower impact on the environment than mechanical compression cooling and heat pumps systems. Moreover, the rising cost of electrical energy added to the issue of climate change are reasons to move towards the development of environmental and sustainable energy technologies.

The absorber and desorber are the key components of absorption heat pumps due to the simultaneous heat and mass transfer processes involved in each one of them [11]. Therefore, the characterization and further advances in the field of absorption and desorption processes implies either the development of more compact absorbers and desorbers or a reduction in the driving temperature of the system for low temperature applications. It is important to stress that the mass transfer in the desorber must be in harmony with the mass transfer in the absorber, therefore, characterization of desorbers must be conducted considering the real operational conditions of the absorption cooling/heating technology under study.

The need of advancing on the development of absorbers has fostered investigation dealing with the intensification of the absorption process employing passive techniques such as the use of compact plate heat exchanger [12,13], inner advanced surface tubes [14], and nanofluids [15,16]. A detailed review of experimental studies on refrigerant absorption enhancement using passive techniques for absorption cooling/heating technologies can be found in [17].

In the case of the desorbers, an increasing number of studies on the characterization of different desorber configurations can be found in the literature. However, there is no evidence of a review that shows advances in design or improved performance techniques for desorbers specifically for absorption heat pumps.

Since the main energy input to the system is through the desorber, its characterization is required to quantify the boiling heat transfer coefficient at different operation conditions for its dimensioning and design. Experimental boiling heat transfer data collected are then used for the development and validation of corre-

* Corresponding author.
E-mail address: mahmoud.bourouis@urv.cat (M. Bourouis).

https://doi.org/10.1016/j.ijheatmasstransfer.2021.121723

lations. The correlations may be dimensional or dimensionless, as well as empirical, semi-empirical, theoretical, or simplified. These correlations are developed in such a way that they involve the effect of parameters selected as control variables in the boiling heat transfer. Control parameters include system pressure, solution inlet temperature, solution mass flow, solution concentration, heat flux, inlet heating fluid temperature or heating surface temperature, thermo-physical properties, and geometrical aspect such as the desorber type, flow configuration, and surface roughness. The number of correlations proposed and available in the open literature to estimate the boiling heat transfer coefficient in different devices has increased over the last years [18–21].

In the literature there are various studies dealing with the boiling process and the proposals of correlations for pure fluids and binary mixtures in pool and forced flow boiling. Those for binary mixtures were obtained using different working fluids to those used in absorption heat pumps. The most recognised correlations for pure fluids in pool boiling and flow boiling can be found in [22,23,32–36,24–31] and in [28,37–40], respectively. In the case of binary mixtures, the most recognised correlations reported for pool and flow boiling can be found in [41,42,51,52,43–50] and in [40,43,53–55], respectively. Moreover, detailed reviews and analysis of those correlations reported to predict pool and flow boiling can be found in [18–21,56]. For instance, Kærn et al. [19] reported a review on the flow boiling correlations for NH_3/H_2O and highlighted that both, convective and nucleate boiling were responsible for the flow boiling process. In agreement with Thonon et al. [57], Kærn et al. [19] concluded that convective boiling suppresses the effect of nucleate boiling when the mass flow is increased, whereas the nucleate boiling contribution was found to be considerable at low mass flows and high heat flux. Mohanty and Das [18] concluded that the correlations available in the literature reproduce the data reported by the same authors fairly well but when reproducing the data of other researchers accuracy is poor. Mohanty and Das [18] explained that bubble dynamic parameters were not considered for the development of those correlations and it would affect their accuracy when reproducing other data. Mohanty and Das [18] and Xu et al. [21] agreed and stressed that much more work had to be done to improve the correlations available for pool and flow boiling of binary mixtures.

To understand and characterise the boiling process in absorption heat pumps, it is important to identify the mechanism responsible for the boiling heat transfer under different circumstances. This has been the focus of various studies in which the main contributors to the boiling process have been identified. However, the contribution of the mechanisms to the boiling process varies depending on the desorber configuration, operating parameters, thermo-physical properties, and others control variables as mentioned before.

This paper aims to evidence the progress in experimental investigations on the boiling process in desorbers, which use advanced designs to enhance heat and mass transfer in conventional and promising working fluids with specific application in absorption heat pumps. Hence, this review identifies, summarises, and discusses the experimental studies carried out on the characterization of desorbers and boiling correlations specifically intended for absorption heat pump technologies. This paper includes a comprehensive scrutiny on the boiling phenomenon in pool desorbers, falling film desorbers, and forced flow desorbers for conventional and promising working fluids. The paper deals in detail with the experimental techniques, test conditions, and the latest advances in desorber design concepts. The dominant mechanisms for boiling enhancement from various studies are presented. Finally, the paper contains ideas for future studies to be carried out for the further development of desorbers used in absorption heat pumps.

2. Thermal conditions and configurations of desorbers in AHP

Depending on the configuration and application, absorption technology for cooling or heating can comprise single-effect absorption systems, multiple-effect or multi-stage absorption systems amongst other types [11]. The driving temperature needed to power the desorber in these systems can vary depending on the working fluid used and the cycle configuration. For example, the driving temperature for a single-effect system can range between 80 °C and 120 °C, for a double-effect system between 130 °C and 160 °C, and for a triple-effect system between 180 °C and 230 °C. Detailed information about the characteristics and driving temperatures of the different absorption heat pumps can be found in [11,58,59].

The mixtures used as working fluids in absorption heat pumps must also meet certain requirements. The mixture should possess favourable transport properties, the refrigerant should have a high heat of vaporization and be miscible within the absorbent for a high range of concentration. Also, the saturation temperature difference between the pure refrigerant and the mixture at the same pressure should be as large as possible. Furthermore, the mixture should be non-toxic, non-explosive, environmentally-friendly, low-cost, and chemically stable over a wide range of temperatures [60].

Desorbers employed in absorption heat pumps can be classified into two groups depending on the energy input mode and the internal flow configuration. Depending on the energy input mode, the desorbers can be direct-fired or indirect-fired. Direct-fired desorbers are those in which the energy reaches the desorber directly and is a result of the combustion of a fossil fuel (for instance, natural gas). Indirect-fired desorbers however, use a thermal fluid to transport the energy from the source to the desorber. The main advantage of indirect-fired desorbers over direct-fired designs is, therefore, that they can use solar energy or residual heat that comes from internal combustion motors, gas turbines, boilers, or any other process.

Regarding internal flow configurations, desorbers can be pool desorbers, falling film desorbers, or forced flow desorbers [61]. Depending on the flow configuration, the boiling process that takes place in the component varies.

The following is a concise description of each desorber and the different flow configurations:

2.1. Pool desorbers

This type of desorber consists of a vessel with a heating surface or a tube serpentine immersed in a large volume of a stagnant mixture. This type of configuration does not rely on flow hydrodynamics and the heat transfer coefficient is not controlled by the amount of refrigerant vapour generated from the base mixture [61]. Moreover, the boiling heat transfer coefficients in this type of desorbers are rather small compared to those of falling film and forced flow desorbers. This is because of the lower heat transfer surface and low flow hydrodynamics. Also, the temperature difference between the heating surface and the saturation temperature of the less volatile component in the binary mixture is lower. This is due to the higher heating surface temperatures required for these desorbers compared to those of others desorbers working with high absorbent concentrations. Since the refrigerant vapour generation depends on the heat flux provided by the heating medium, the boiling process in pool desorbers is mainly influenced by nucleate boiling. Furthermore, studies available in the literature usually focus on the effect of the heat flux, the system pressure, and the solution concentration in the boiling process.

The experimental studies found in the open literature dealing with the performance of pool desorbers for absorption heat pumps are reviewed in sub-Section 3.1.

2.2. Falling-film desorbers

This type of desorber may appear both, horizontal or vertical orientation. The latest advances have added plates with extended surfaces to achieve more compact designs. In the case of the horizontal configuration, the solution enters the desorber through a distributor placed at the upper section and then flows in a thin falling-film along horizontal heating tube surfaces. The heating fluid flowing in the tubes provides the energy required to generate refrigerant vapour from the solution that is flowing over the surface of the tubes. Although this configuration usually offers high boiling heat transfer coefficients, the key factors that affect the boiling process are the diameter and wetting of the tube, and so these are parameters that should be carefully addressed. In the case of vertical orientation desorbers, there are designs where the solution may flow as a falling-film over the inner surface, or the outer surface of the inner tubes. Tube diameter and surface wetting are also factors to be considered and optimised, since solution flow hydrodynamics affects the boiling heat transfer. Therefore, given the effect of the solution flow on refrigerant boiling, the temperature gradient between the refrigerant saturation temperature and the heating fluid temperature may be inferior. This means that both, convective boiling, and nucleate boiling may be responsible for the boiling heat transfer coefficient depending on the operating conditions as evidenced in sub-section 4.2. Studies found in the open literature relate to the effect of the heat flux, system pressure, solution flow, and solution concentration in the boiling process. The experimental studies found in the open literature dealing with the performance of falling-film desorbers for absorption heat pumps are reviewed in sub-Section 3.2.

2.3. Forced flow desorbers

This type of desorbers can also be manufactured with both, horizontal and vertical tube orientation. Compact designs using plates with extended surfaces or membranes are also included in this section. In the case of vertical tube orientation, the solution enters the desorber from the bottom of the unit and flows upwards exchanging heat with the heating fluid flowing in a counter-current configuration. In the case of horizontal tube orientation, the solution enters the desorber from one side of the unit, while the heating fluid flows in a counter-current configuration. During the heat exchange, part of the refrigerant in the solution boils on once it reaches the saturation temperature required and leaves the desorber. In forced flow desorbers, the cross-sectional flow areas and flow hydrodynamics are key factors to be considered. Moreover, this configuration also offers a small temperature gradient between the refrigerant saturation temperature and the heating fluid temperature and high boiling heat transfer coefficients. The literature relevant, indicates that convective and nucleate boiling can coexist during the boiling heat transfer process depending on the operating conditions as discussed in sub-Section 3.3. Investigations available in the literature on forced flow boiling processes deals with the effect of the heat flux, system pressure, solution flow and concentration, heating fluid temperature, heating fluid flow and the cross-sectional flow area in the boiling process. The experimental studies found in the open literature dealing with the performance of forced flow desorbers for absorption heat pumps are reviewed in sub-Section 3.3.

3. Experimental investigations

In this section, the experimental investigations into desorbers used in absorption heat pumps are identified and analysed. The investigations included the correlations available in the literature on desorption processes working with different fluids specifically obtained for absorption heat pumps. These investigations are classified and presented in the following three sections as determined by the flow configuration of the process.

3.1. Pool boiling

The initial studies available in the literature were carried out on desorbers with the pool boiling configuration, because of the simple design involved. Charters et al. [62] reported the nucleate boiling heat transfer of H_2O/LiBr and pure water using a smooth copper tube as a heating medium in a vertical evaporator. The authors correlated and proposed dimensionless equations based on the Nusselt number, the Prandtl number, and the Stanton number to estimate the H_2O/LiBr film coefficient. Later on, Varma et al. [63] evaluated the pool boiling of H_2O/LiBr using three stainless steel tubes of different diameters. The authors also quantified the effect of system pressure, heat flux, and solution concentration. Results in Fig. 1a show that as the solution concentration increases and the heat flux decreases, the boiling heat transfer coefficient drops. The authors also noted that the solution concentration affected boiling heat transfer more than heat flux and system pressure did. Moreover, the effect of internal tube diameter on boiling heat transfer was found to be negligible, (see Fig. 1b).

Inoue et al. [64] evaluated the nucleate boiling of NH_3/H_2O using a horizontal wire as a heating medium. The authors show in Fig. 2 that the pure fluids of the binary mixture present higher heat transfer coefficients than those of the mixture, when the concentration is in a range between 0.3 and 0.7 when heat transfer drops to a minimum. The authors also tested some correlations for boiling heat transfer available in the literature and evidenced that some of the correlations tested adequately estimated the boiling heat transfer of pure ammonia and water but failed to reproduce the boiling heat transfer of the NH_3/H_2O mixture in a wide range of concentrations.

Arima et al. [65] quantified the pool boiling heat transfer of NH_3/H_2O on a horizontal surface and used a block, located at the bottom of the test vessel, as a heating medium. The experimental study pointed towards similar conclusions to those reported by Inoue et al. [64] regarding the effect of solution concentration on heat transfer. Moreover, the authors proposed a fitted correlation to estimate the heat transfer coefficient, showing acceptable agreement against experimental data mainly at mixture concentrations below 0.9.

Táboas et al. [66] conducted a review on boiling heat transfer correlations to test their accuracy to predict experimental data available in the literature for nucleate boiling of a NH_3/H_2O mixture and its pure fluids. In this study, the data reported by Inoue et al. [64] and Arima et al. [65] were used to test the selected correlations. Results showed that the available correlations failed to make a reasonable prediction of heat transfer coefficient over a wide range of solution concentrations. Therefore, the authors developed a new NH_3/H_2O boiling heat transfer correlation with an accuracy of ±40% of error. This correlation was based on the correlations reported by Schlunder [41] and [42,57] with fitted parameters. Later on, Inoue and Monde [67] published two boiling heat transfer correlations for NH_3/H_2O based on the experiments previously obtained in [64] with an accuracy of ±20% of error. The correlations are valid for all the concentration range and for heat fluxes below 1000 kW m^{-2}.

Sathyabhama and Ashok Babu [68,69] presented an experimental and visual observation study on NH_3/H_2O pool boiling heat transfer in a stainless-steel vessel using two sight glasses. The solution was heated by a rod heater placed vertically at the bottom of the vessel. The authors tested the effect of the solution concentration, pressure, and heat flux on the boiling heat transfer and showed that heat transfer dropped drastically when the ammonia

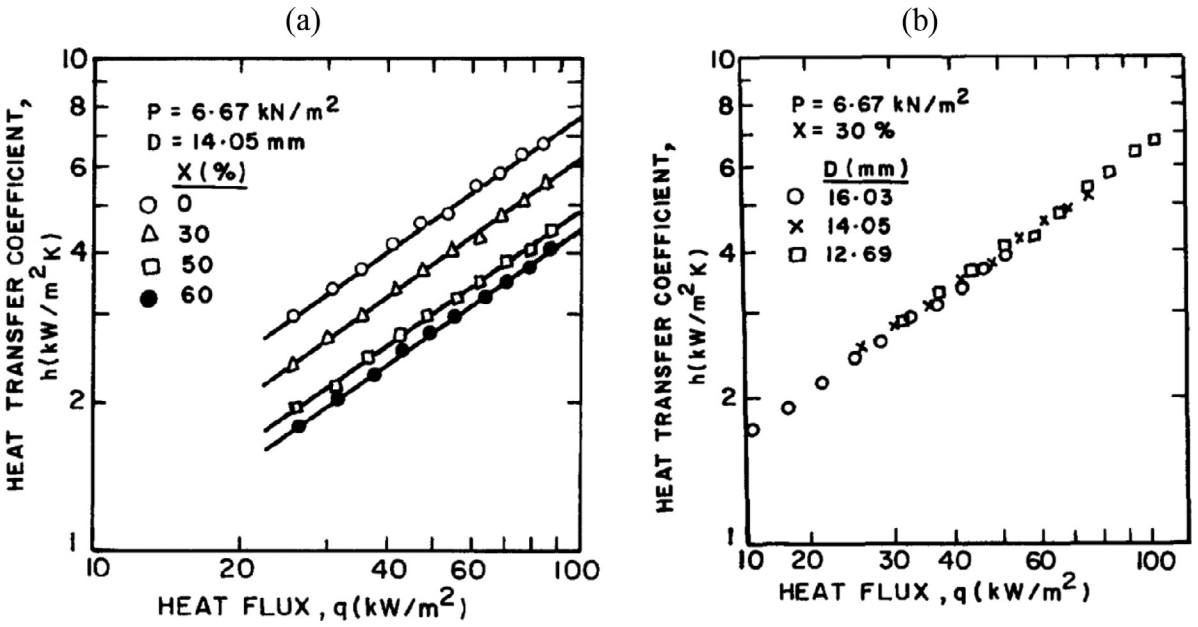

Fig. 1. Effect of (a) solution concentration and heat flux, and (b) tube diameter on the pool boiling heat transfer coefficient for H2O/LiBr [63].

concentration was increased from 0 to 0.1, then it decreased slightly. They also showed that the higher the heat flux and pressure, the higher the heat transfer. Furthermore, the visual observation study revealed that, as observed by Inoue et al. [70], bubble generation frequency rose on increasing heat flux and pressure. Finally, the authors improved the correlations reported by Calus and Rice [71] and Stephan and Korner [72] using the data obtained in this research together with those from Arima et al. [65] and Inoue et al. [64]. The corresponding correlations achieved accuracies of ±18% and ±16%, respectively.

In a related study carried out in the same test facility used in previous studies, Sathyabhama and Ashok Babu [73] reported how boiling heat transfer of NH_3/H_2O was affected by adding mass fractions of LiBr. Results showed that NH_3/H_2O boiling heat transfer rises drastically when mass fractions of LiBr are increased from 0 to 0.5 at a pressure of 4 bar. However, this effect decreases as system pressure increases. Visual observation experiments also evidenced that the addition of LiBr facilitated clusters of small-sized bubbles and higher bubble flow frequencies.

Following up the results in [70], Inoue and Monde [74] evaluated the effect of the surfactant Surflon S-451 on NH_3/H_2O boiling heat transfer in the same test facility previously used. The visual observation study showed similar bubble behaviour in terms of bubble size and departure frequency when the surfactant was added, similar to the studies by Inoue et al. [70]. The enhancement rate achieved by adding 1000 ppm of surfactant to an ammonia concentration of 0.1 was up to 0.36.

Following up their previous investigations, Sathyabhama and Ashok Babu [75] evaluated NH_3/H_2O boiling heat transfer by adding mass fractions of $LiNO_3$. Results in Fig. 3 indicate that NH_3/H_2O boiling heat transfer increases up to 40 kW m^{-2} K^{-1} on increasing the mass fractions of $LiNO_3$ from 0 to 0.5 mainly a low NH_3 mass fractions.

In one of the few studies carried out using nanofluids in desorbers, Jung et al. [76] evaluated the effect of adding AL_2O_3 nanoparticles to H_2O/LiBr mixtures in pool boiling heat transfers. The test section consisted of a vessel at vacuum conditions and heated by a plate heater. Results showed that the boiling heat transfer coefficient decreased on increasing the AL_2O_3 concentration in the base mixture. The authors also evidenced that the drop in the heat transfer coefficient was more pronounced when the base mixture concentration was increased. This negative effect was attributed to nanoparticles being deposited on the plate heater which consequently reduced boiling nucleation.

Han et al. [77] investigated the effect of using ultrasonic waves on H_2O/LiBr pool boiling process in a glass vessel. The authors concluded that higher desorption rates could be obtained by using an ultrasonic transducer rather than that of an electric heating rod with the same power (see Fig. 4). Desorption rates of up to 5 g m^{-2} s^{-1} were obtained at the highest heating temperature set, for a solution concentration of 53%, and using a 20 W ultrasonic device. Solution concentrations higher or lower than 53% showed lower desorption rates. The authors suggested that the improvement obtained with the ultrasonic transducer waves could be due to the combination of micro disturbances, acoustic streaming, and cavitation effects.

To conclude this sub-section, it is worth note that most of the studies in pool boiling found in the literature deal with the characterization of pool boiling in basic configurations using conventional working fluids, whereas fewer studies reported the use of enhancement techniques. For instance, only one study reported the effect of additives on pool boiling [78], one study was found using nanofluids [76], and one applied ultrasonic waves [77].

Table 1 provides a compendium of the experimental studies carried out in pool boiling conditions using conventional and promising working fluids for absorption heat pumps.

3.2. Falling film boiling

Investigations reported in the literature showed that there was higher heat transfer performance in desorbers designed in falling-film boiling mode than those in pool boiling mode, at low wall superheating temperatures [79]. Falling-film desorbers arouse special interest because they have the potential to improve flow hydrodynamics when advanced surfaces and compact design concepts are used.

Tuzla et al. [80] conducted visual observation experiments to analyse the inception of bubble nucleation in falling-films with H_2O/glycerol mixtures. The desorber consisted of a vertical glass tube with an internal stainless-steel tube as a heating medium.

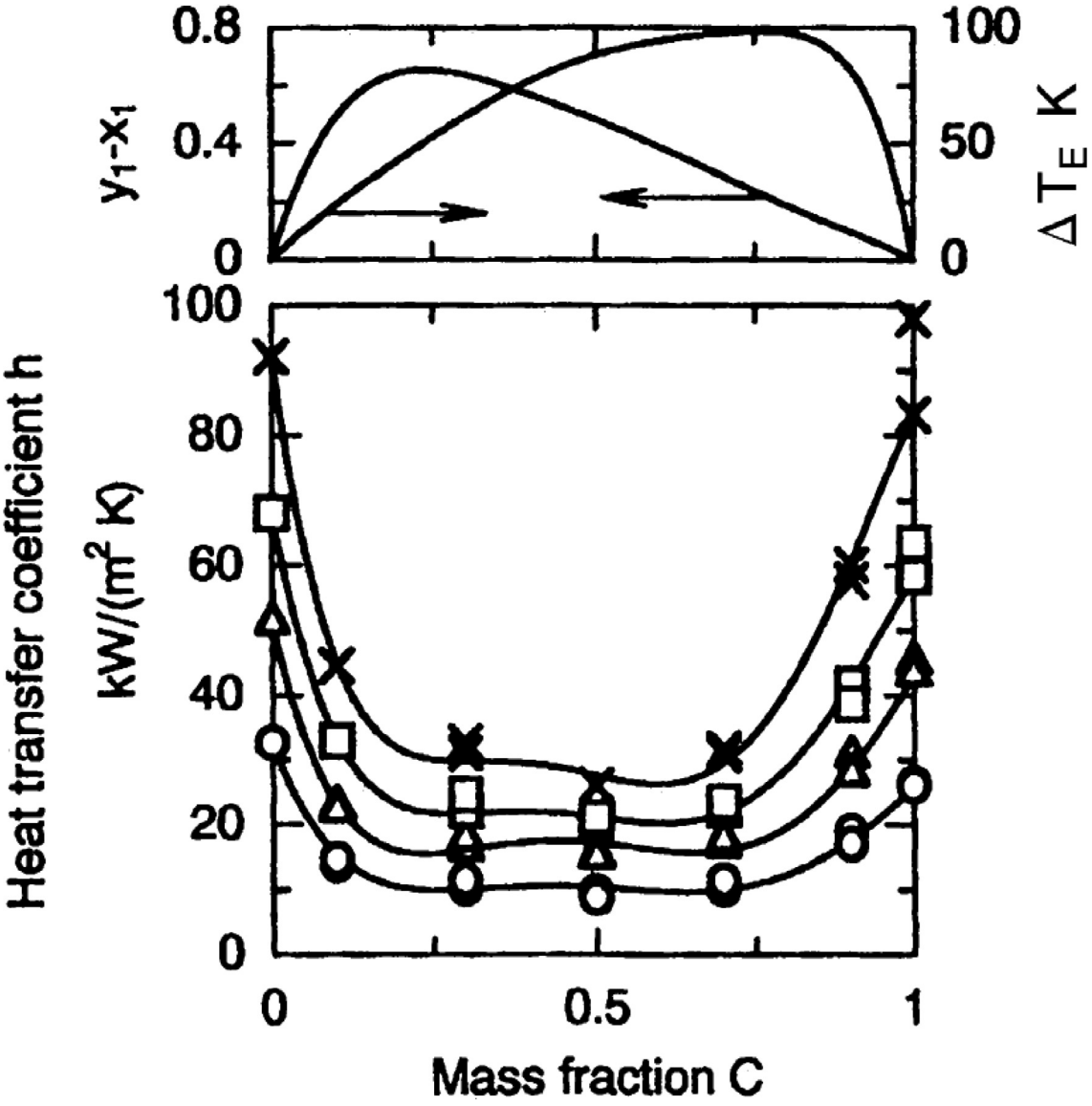

Fig. 2. Mass fraction versus heat transfer coefficient for NH_3/H_2O [64].

The authors show in Fig. 5 that the heat transfer coefficient of the working fluid along the steel tube tends to decrease when the subcooled mixture is heated until its saturation temperature. It then tends to increase when the temperature is increased beyond saturation temperature. The authors also found that, wall superheat for boiling inception increases on decreasing system pressure, mass flow, and glycerol concentration.

Shi et al. [81,82] carried out an experimental study on H_2O/LiBr boiling heat transfer in falling-film mode. The desorber consisted of a vertical tube heated by an electrical resistance placed around the tube. Results indicated that boiling heat transfer increased when the heat flux was increased from 10 kW m^{-2} to 25 kW m^{-2} and the volumetric flow was increased from 9 ml s^{-1} to 12.5 ml s^{-1}. Also, the heat transfer coefficient was found to decrease on increasing the mass fraction of LiBr since this facilitated the boiling of the most volatile component (see Fig. 6). In these experiments, heat transfer ranged from around 0.75 kW m^{-2} K^{-1} to 1.66 kW m^{-2} K^{-1}. The authors also compared heat transfer performance using a falling-film vapour desorber and a submerged desorber. The comparison showed a much higher heat transfer coefficient in the case of the falling-film desorber.

Later on, Determan and Garimella [83] reported the NH_3/H_2O boiling process in a microchannel desorber. Fig. 7 shows that the desorber consisted of microchannel tubes located in various square arrays forming 5 passes of 16 tube rows (each row with 27 tubes). In this test section, a glycol/water solution, used as a heating medium, flowed upwards through the tube array with pressure drops occurring between 11 kPa and 30 kPa, while an NH_3/H_2O falling solution flowed downwards. In this study, the overall heat transfer coefficient ranged from 388 W m^{-2} K^{-1} to 617 W m^{-2} K^{-1} when the NH_3/H_2O mass flow was increased. In this design, the wetted area occurring during desorption was subjected to evaluation and it was found to improve during the highest mass flows tested and better-wetted area fractions were obtained between the third pass and the fifth one.

Lazcano-Véliz [84] tested a horizontal bundle of tubes operating as a generator for a H_2O/LiBr absorption heat transformer. This study was focused on identifying the optimum mass flow to obtain the best wetting area. As a result, the mass flow of 0.025 kg s^{-1} m^{-1} was identified as the optimum value. Keinath et al. [85] and Delahanty et al. [86] evaluated the NH_3/H_2O desorption process in new concepts of compact plate desorber-rectifiers.

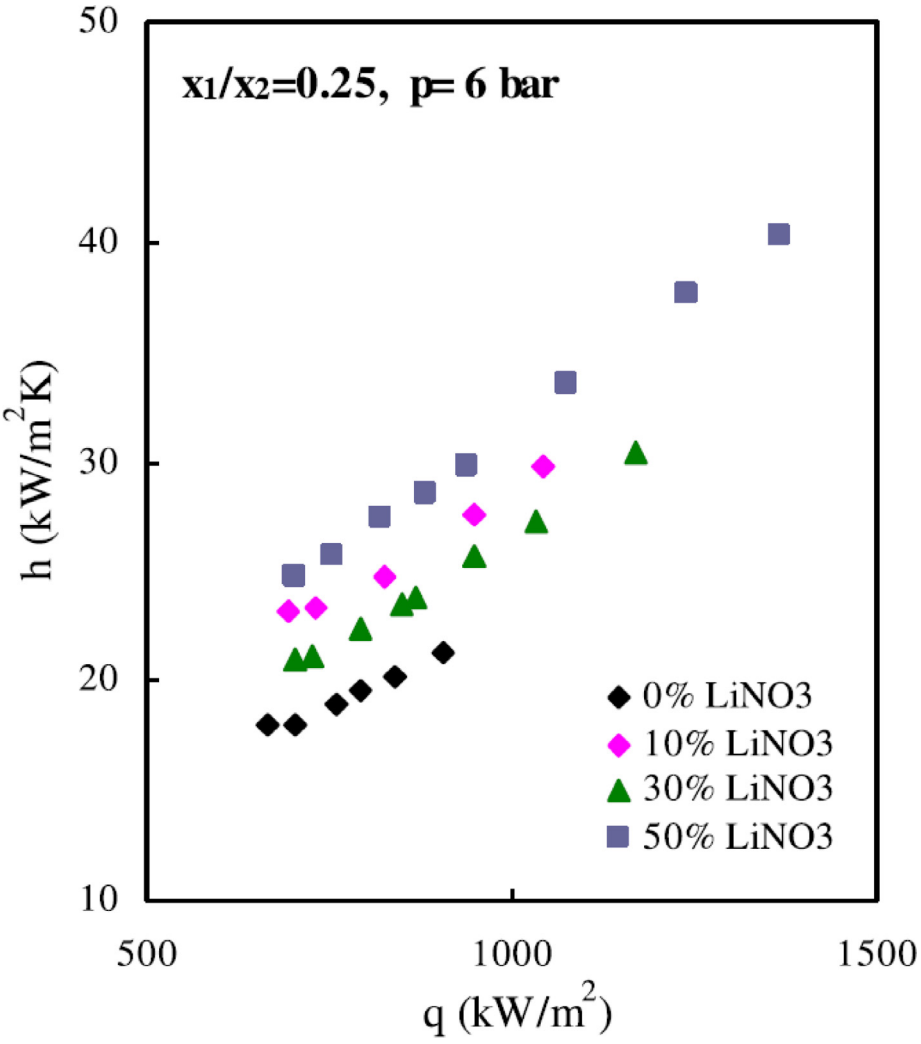

Fig. 3. Boiling heat transfer coefficient vs heat flux and $LiNO_3$ mass fraction [75].

Keinath et al. [85] tested a desorber-rectifier with the overall dimensions 287 mm × 171 mm × 83 mm (see Fig. 8). This study presented how the solution flow rate and the heating fluid temperature affected the desorption rate and heat duty. Results indicated that the desorption rate increased up to 12.5 kg h^{-1} when the solution flow and heating temperature were increased. Also, as the heating fluid temperature increased, the desorber and rectifier heat duty rose to 7.5 kW and 2.47 kW, respectively. However, at a heating fluid temperature of 190 °C, the desorber-rectifier duty dropped as the desorption rate increased.

Olbricht et al. [87] studied the H_2O/LiBr heat transfer in a desorber with a horizontal bundle of 80 tubes. The authors reported that the heat transfer improved as the solution flow rate increased. As in absorbers, the wettability of the tubes was identified as the limiting factor with respect to achieving a higher heat transfer coefficient. Mortazavi et al. [88] tested the H_2O/LiBr desorption process in a compact plate-and-frame desorber operating at conditions for absorption chillers driven by low temperature heat. The desorber consisted of a plate with extended structures made of copper sheets as shown in Fig. 9a. In this study, the authors discussed the effects of wall superheating temperature, solution mass fraction, and solution mass flow on the desorption rate. Also, the authors compared the desorption rates obtained in their study with those reported in the literature involving other desorber designs. As Nasr Isfahani et al. [89] pointed out, the authors also distinguished two boiling modes, direct diffusion and nucleate boiling. The authors concluded that direct diffusion takes place at low wall superheat temperatures and at low solution flows. Moreover, the nucleate boiling is more evident at high super wall temperatures when a sharper increase in boiling heat transfer occurs as compared to that of direct diffusion (Fig. 9b). Finally, the authors evidenced that the desorber design tested, provided desorption rates higher than those in the data reported by Kim and Kim [79] at lower mass flows.

Lazcano-Véliz et al. [90,91] reported the wetting and heat transfer performance of a concentric helical generator for an H_2O/LiBr absorption heat transformer. Their results showed that the heat transfer coefficient increased up to 5541 W m^{-2} K^{-1} on decreasing film thickness. Moreover, film thickness decreased when mass flow was decreased. The authors explained that the reason for this behaviour was due to a more uniform film flow over the coil occurring at low mass flows.

Hu et al. [92] presented LiBr/H_2O boiling tests carried out on a novel plate generator for absorption heat pumps, working in falling-film mode. The test section consisted of a three-channel plate generator with four stainless steel plates. In this generator, which included 120° of arc horizontal columns welded to the central channel, the solution flowed downwards in the central channel, while the heating water flowed upwards in the side channels. Results in this study showed that wettability was gradually com-

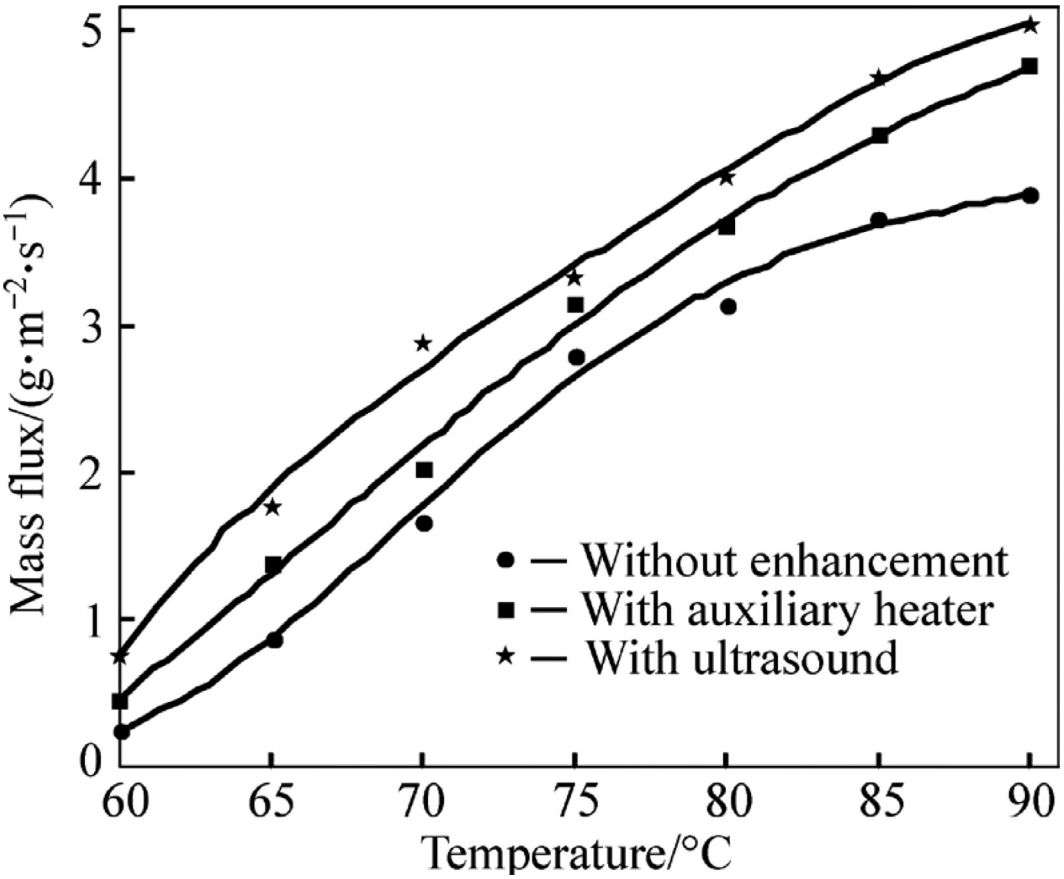

Fig. 4. Desorption mass flux versus heating temperature by [77].

pleted as the solution mass flow and heating flow temperature increased. Regarding the heat transfer coefficients, these ranged from 735 W m^{-2} K^{-1} to 856 W m^{-2} K^{-1}.

Staedter and Garimella [93,94] presented a report on the performance of a new design of an NH_3/H_2O desorber-rectifier. As shown in Fig. 10, the component was formed by plates with internal micro-channels and various trays, along which the solution mixture flowed downwards and the ammonia vapour upwards. The effect of solution pressure, solution flow, solution concentration, and solution temperature on the desorption process was evaluated. Results showed solution heat transfer coefficients as high as 3250 W m^{-2} K^{-1} at an ammonia mass fraction of 43%, and mass transfer coefficients as high as 0.0022 m s^{-1}. According to the authors, favourable hydrodynamics for heat and mass transfer are a key aspect of the present design. In a similar study, Staedter and Garimella [95] proposed a tube desorber driven by two passes of flue gases for direct gas-coupling applications (see Fig. 11). Results showed low gas side heat transfer coefficients which limit heat transfer in the desorber. The liquid mass transfer coefficient was up to 0.00085 m s^{-1}.

In an absorption chiller test facility, Keinath et al. [96] tested two plate desorber-rectifier designs fed by NH_3/H_2O. According to the authors, the tests involved a vertical column configuration and a branched tray configuration. However, no details were reported regarding the operating test conditions of the study or the size/heat transfer area of either component. Results indicated that the branched tray design provided higher heat duties and refrigerant flows than the vertical column, with heat duty up to 3.6 kW and refrigerant flow up to 0.00178 kg s^{-1}.

Hernández-Magallanes and Rivera [97] evaluated $NH_3/LiNO_3$ falling-film boiling on a helical coil generator installed in an absorption system test facility. In this generator, the heating water flowed downwards inside the coil while the solution flowed in falling-film mode over the coil. This study showed boiling heat transfer coefficients reaching up to 270 W m^{-2} K^{-1} and refrigerant vapour flow rates up to 0.11 kg s^{-1} at the highest the heat flux and solution mass flux fixed.

Delahanty et al. [98] continued the research from Keinath et al. [96] on NH_3/H_2O boiling but using two new desorber-rectifier designs: a new vertical column and a new branched tray design as shown in Fig. 12. This study also showed that the tray configuration desorber-rectifier provided higher heat transfer characteristics than that of the vertical column configuration. The desorber duty and solution heat transfer coefficients reported for the tray design reached up to 0.8 kW and 11,900 W m^{-2} K^{-1} at the highest solution concentration and flow set, respectively. This study also included a proposal for a new boiling heat transfer correlation.

Finally, Hu et al. [99] evaluated the performance of a $LiBr/H_2O$ falling-film generator concept which uses water as a heating medium in a counter-current flow. As shown in Fig. 13, the generator proposed is a detachable device, with two entwined modules. The central channels can be separated by moving the two modules upwards. This study demonstrated that the boiling heat transfer and mass transfer coefficients increased up to 0.64 kW m^{-2} K^{-1} and 7.8 $\times$ 10^{-5} m s^{-1}, respectively, the heat flux was increased. However, the effect of the solution mass flux on the boiling heat transfer was not clear, which means that nucleate boiling was predominant.

To conclude this sub-section, it is important to note that tube wetting should be carefully addressed when designing falling-film desorbers. Equally important is that diffusion, convective, and nucleate phenomena appear to be the main contributors to boiling

Table 1
Compendium of the experimental studies on pool boiling desorbers for absorption heat pump systems.

Reference	Test section	Working fluids	Test condition ranges	Note
[62]	Vertical evaporator with an internal smooth cooper tube of 16 mm OD and 0.25 m in length.	H_2O/LiBr and pure H_2O	For the H_2O/LiBr solution: P (9.3–18.7 kPa), X (25–56.5%), T_w-T_s (8.8–18.8 °C), $\dot{Q}$/A (3.24–32.57 kW m^{-2}), For the pure water: P (9.3–101.4 kPa), T_w-T_s (3.8–12.6 °C), $\dot{Q}$/A (2.62–44.17 kW m^{-2})	Proposal of Correlation under nucleate boiling conditions.
[63]	Vertical cylinder made of stainless steel with an internal horizontal stainless-steel tube of 0.24 m in length.	H_2O/LiBr	P (4–9.33 kPa), X (0–60%), $\dot{Q}$/A (15–108 kW m^{-2}), tube diameter (12.69 mm, 14.05 mm, and 16.03 mm OD)	X affects H_2O/LiBr boiling more than P and $\dot{Q}$/A.
[64]	Vessel with horizontal platinum wire (0.3 mm in diameter, 37 mm in length) located below the solution level.	NH_3/H_2O	P (400–700 kPa), X (0–100%), $\dot{Q}$/A (400–1500 kW m^{-2})	The boiling heat transfer of NH_3/H_2O mixtures becomes drastically lower than that of both pure components.
[65]	Vessel (200 mm ID and 360 mm in height) with a heating block at the bottom.	NH_3/H_2O	P (200–1500 kPa), X (0–100%), $\dot{Q}$/A (500- 2000 kW m^{-2})	It includes visual observation experiments. Proposal of correlation for heat transfer with an acceptable agreement with respect to experimental data at mass fractions below 0.9.
[68,69]	Stainless steel vessel of 80 mm in diameter and 200 mm long with rod heater. Heating length of 20 mm.	NH_3/H_2O	P (400–800 kPa), X (0–30%), $\dot{Q}$/A (360–1200 kW m^{-2})	It includes visual observation experiments. Heat transfer drops drastically when ammonia fraction is increased from 0 to 0.1, then it decreases slightly. Proposal of Correlation.
[73]	Stainless steel vessel of 80 mm in diameter and 200 mm long with rod heater. heating length of 20 mm.	$NH_3/(H_2O+LiBr)$	P (400–800 kPa), X (15–30%), X_{LiBr} (0–30%) $\dot{Q}$/A (360–1200 kW m^{-2})	It includes visual observation experiments. NH_3/H_2O boiling heat transfer increases on increasing the mass fractions of LiBr.
[74]	Vessel with horizontal platinum wire (0.3 mm in diameter, 37 mm in length) located below the solution level.	NH_3/H_2O with surfactant	P (400 kPa), X (10–90%), Xs (0–3500 ppm), $\dot{Q}$/A (10–1000 kW m^{-2})	It includes visual observation experiments. Enhancement rate improved up to 0.36 by adding 1000 ppm of surfactant.
[75]	Stainless steel vessel of 80 mm in diameter and 200 mm long with rod heater. heating length of 20 mm.	$NH_3/(H_2O+LiNO_3)$	P (400–800 kPa), X (15–30%), X_{LiNO3} (10–50%) $\dot{Q}$/A (421–2321 kW m^{-2})	NH_3/H_2O boiling heat transfer increases on increasing mass fractions of $LiNO_3$ mainly at low NH_3 mass fractions.
[76]	Vessel with a horizontal plate heater of 2 kW	$H_2O/(LiBr+Al_2O_3)$	P (4 kPa), X (3–10%), T_w-T_s (1–60 °C), $\dot{Q}$/A (0–900 kW m^{-2}), Al_2O_3 (0.01–0.1%V)	The boiling heat transfer coefficient decreases on increasing the AL_2O_3 concentration in the base mixture at the studied conditions.
[77]	Vessel with ultrasonic transducer and an electric heating rod	H_2O/LiBr	T_w (60–90 °C), X (50–58%), heating power (20–60 W)	Higher desorption rates by using an ultrasonic transducer rather than an electric heating rod.

P (inlet solution pressure), X (solution concentration), Xs (inlet surfactant concentration), xv (mean vapour quality), T_i (inlet solution temperature), T_w (wall surface temperature), T_s (saturation temperature of the fluid), T_H (inlet heating fluid temperature), $\dot{m}$ (solution mass flow), Γ (solution mass flow per unit of length), G (solution mass flow per unit of area), G_H (heating fluid mass flow per unit of area), V (Solution volumetric flow), V_H (Heating fluid volumetric flow), $\dot{\mathbf{Q}}$ (heat transfer rate), $\dot{\mathbf{Q}}$/A (heat transfer rate per unit of area).

heat transfer, but that their predominance would depend on the operating conditions.

It is also clear that most of the studies on falling-film boiling process, found in the literature, involve proposed compact desorber designs which characteristically use conventional working fluids. Furthermore, no studies have been found regarding the use of additives or nanofluids to enhance heat and mass transfer in this type of desorber.

Table 2 provides a compendium of the experimental studies carried out regarding falling-film boiling conditions where conventional and promising working fluids are used for absorption heat pumps.

3.3. Forced flow boiling

There have been more investigations regarding forced flow boiling lately thanks to developments in membranes and compact plate heat exchangers. These components use advanced surfaces which allow for better flow hydrodynamics and an improved heat transfer area.

Initial studies included that of Jurng and Woo Park [100] who reported on a H_2O/LiBr desorber heated by a gas burner. The main results showed that the refrigerant desorbed, and the solution concentration difference increased linearly with the heat input at the operating conditions set for the study. Rivera and Best [101] investigated the boiling process in a smooth vertical tube working with NH_3/H_2O and $NH_3/LiNO_3$ mixtures. In the latter case, the solution flowed upwards through the smooth vertical tube and was heated by a spiral electrical resistance located along the tube. This study showed that the average heat transfer coefficient increased when the solution concentration and the heat flux were increased, but mainly at low mass flows. The authors also evidenced that heat transfer values using a NH_3/H_2O mixture were around two and/or three times higher than the values obtained using a $NH_3/LiNO_3$ mixture. From their experiments, the authors also reported correlations the local heat transfer coefficients of the NH_3/H_2O and $NH_3/LiNO_3$ mixtures which registered mean deviations of 25% and 16%, respectively.

One of the first studies that reported on the use of membrane-based desorbers is that of Riffat et al. [102]. In the study, the

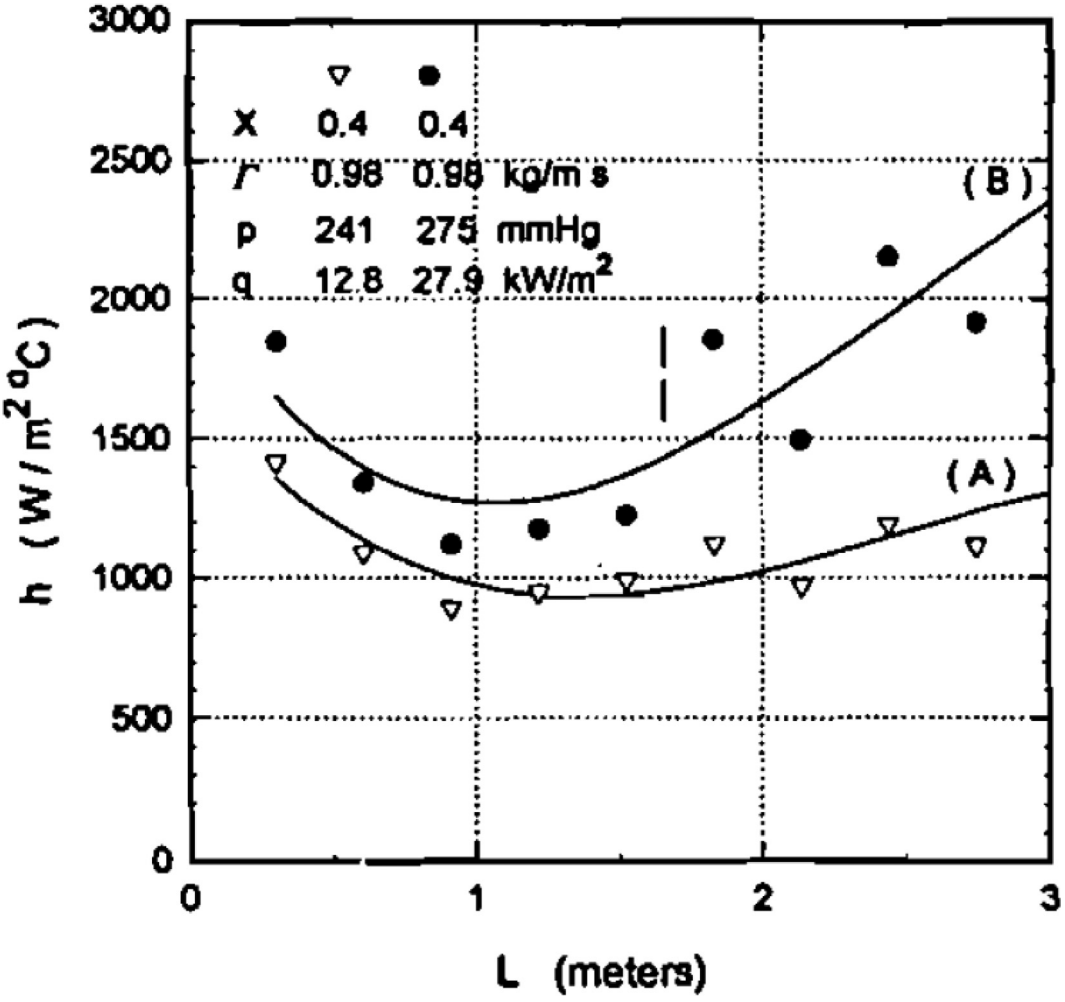

Fig. 5. Local heat transfer coefficient profiles with and without boiling for H_2O/glycerol [80].

authors evaluated the desorption rate of H_2O/Potassium formate working in a membrane-based desorber-condenser. In the test section, a polymer membrane and a tubular silicon membrane were evaluated. In this component, the solution was previously heated, so that the water diffused through to the other side of the membrane where it encountered lower pressure and evaporated. The study showed that the desorption rate increased when solution pressure and concentration were reduced. Results also demonstrated that desorption rates were higher with the tubular silicon membrane than with the polymer membrane. Moreover, the authors evidenced that desorption rate could be improved up to five times that with H_2O/Potassium formate by adding caesium formate to the base mixture.

Khir et al. [103,104] reported on boiling heat transfer using NH_3/H_2O in a stainless steel vertical double pipe. The solution flowed upwards through the inner tube and water, i.e., the heating medium, flowed in a counter-current configuration in the outer annulus. An analysis was carried out to see how boiling heat transfer was affected by solution concentration, mass flow and heat flow. Also, the authors tested the accuracy of any correlations available in the literature to be able to replicate the experimental data. Results evidenced that for a NH_3/H_2O mixture, working at the given operating conditions, the effect of heat flow and mass flow was greater than the effect of the solution concentration. The authors concluded that the correlation reported by Mishra et al. [54] was adequate enough to predict NH_3/H_2O boiling heat transfer within ±12% of error at the conditions of the study.

Thorud et al. [105] tested H_2O/LiBr desorption carried out in a membrane-based desorber in order to evaluate desorption rate at different solution concentrations, pressure differences across the membrane, and wall superheating temperatures. Results showed that an increase in wall superheating temperature and a pressure difference in the membrane resulted in higher desorption rates. The authors also evidenced that desorption rate increased when the LiBr mass fraction was decreased.

Marcos et al. [106] presented a study of the boiling heat transfer coefficient and pressure drop in a plate heat exchanger working as a desorber and integrated into an air-cooled double effect H_2O/LiBr absorption prototype. In this study, thermal oil acted as the heating medium in the plate heat exchanger. The oil was previously heated by an electrical resistance and flowed upwards. The solution mixture was configured to flow co-currently. To estimate the boiling heat transfer coefficient, the authors defined two zones, the first was for liquid/liquid heat transfer and the second was for liquid/liquid-vapour heat transfer. The heat transfer for zone one was determined using the correlations reported by Thonon [107] and Hewitt and Shires [108]. For zone two, the heat transfer was estimated by applying the heat transfer resistance equation to this part of the desorber. Results evidenced that boiling heat transfer in zone two could reach a value four times higher (around 5.2 $kW.m^{-2}\ K^{-1}$) than that of zone one depending what correlations were used for a single phase. Results also evidenced that the quality of the refrigerant during the boiling process ranged from 2% to 6% which meant that most of the boiling process was a

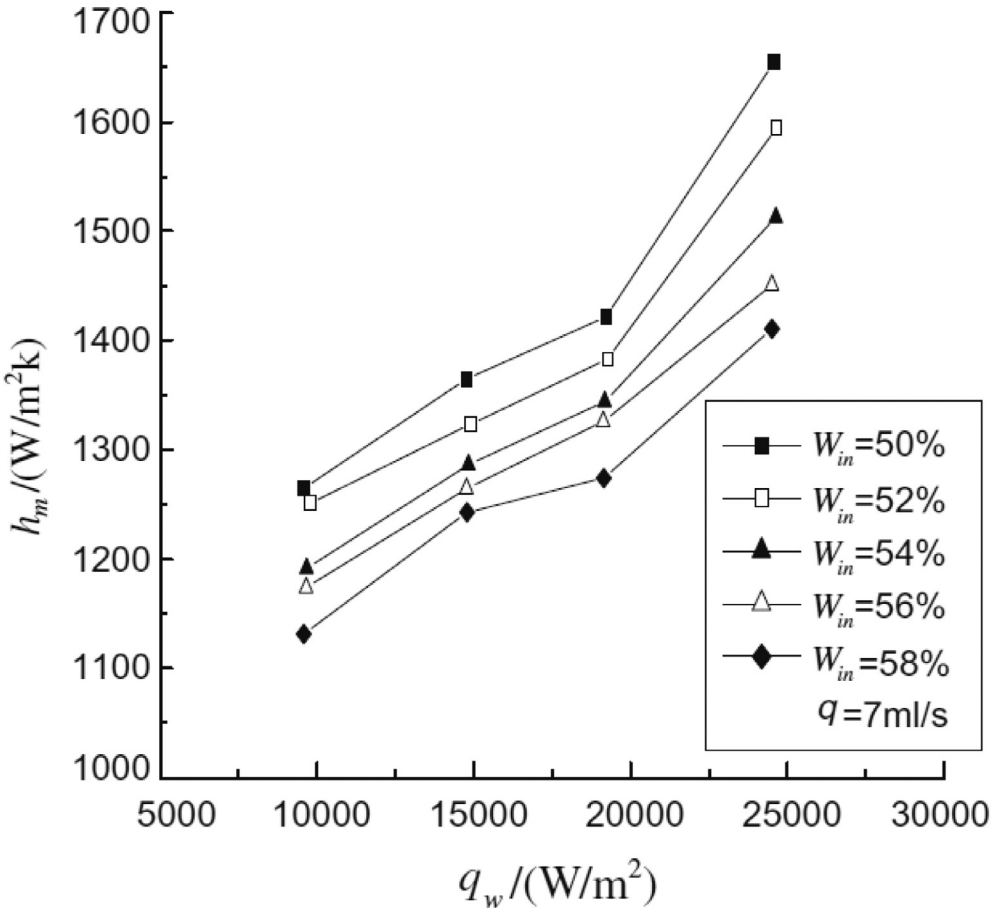

Fig. 6. Boiling heat transfer coefficient as a function of heat flux for various mass fractions of LiBr [82].

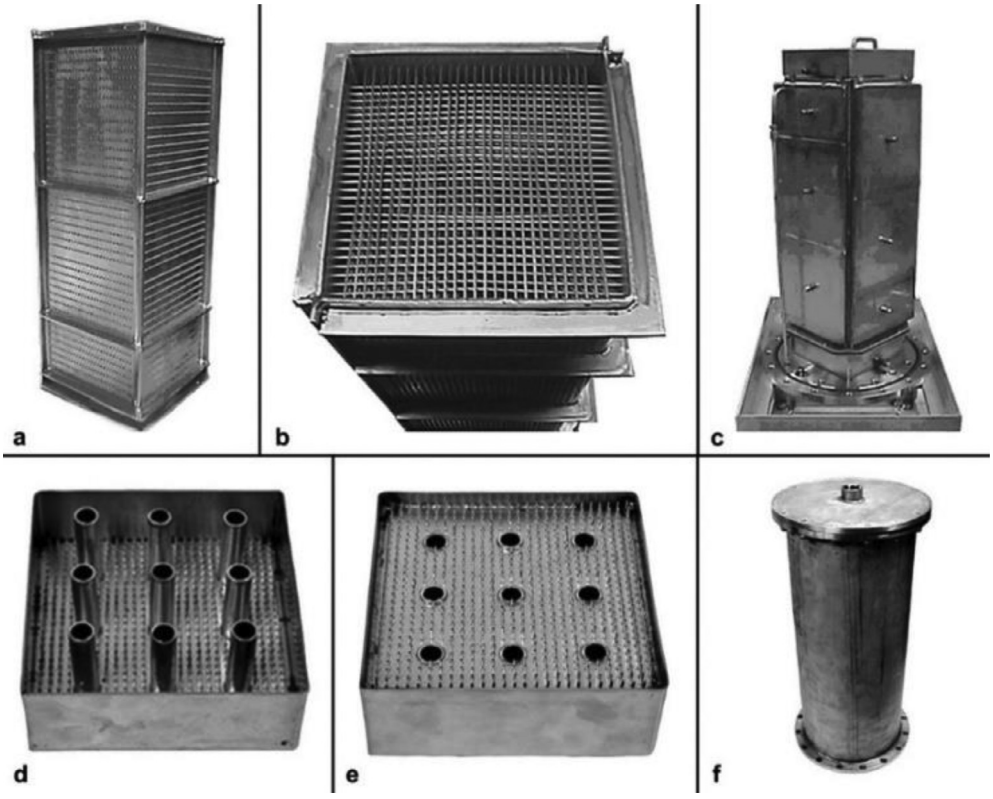

Fig. 7. Prototype of desorber with microchannels [83].

Table 2
Compendium of the experimental studies on falling film desorbers for absorption heat pumps.

Reference	Test section	Working fluids	Test condition ranges	Note
[80]	Vertical glass tube with an internal stainless-steel tube of 38 mm OD and 2.9 m of heated length.	H_2O/Glycerol	P (3.33–57.86 kPa), X (40–60%), Γ (0.2–1.3 kg s^{-1} m^{-1}), T_w-T_s (12–30 °C), $\dot{Q}$/A (12.7–28 kW m^{-2})	It includes visual observation experiments. Boiling inception increases with decreasing system pressure, mass flow, and glycerol concentration.
[81,82]	Stainless steel vertical tube with 25/21 mm OD/ID and 760 mm in length.	H_2O/LiBr	P (97.25 kPa), X (49.5–58%), V (7–14 ml s^{-1}), $\dot{Q}$/A (5–25 kW m^{-2})	Better heat transfer performance in a falling film generator when compared to that in a submerged generator. Proposal of Correlation.
[83]	Stainless steel microchannel heat exchanger with 5 passes of 16 tube rows (each one with 27 tubes) for a surface area of 1.5 m^2.	NH_3/H_2O	P (664.7 kPa), T_H (99.4 °C), X (15–30%), G (0.0188–0.0339 kg s^{-1}), G_H (0.11–0.19 kg s^{-1}), $\dot{Q}$ (5.4–17.5 kW)	Overall heat transfer coefficient improves almost linearly on increasing the NH_3/H_2O mass flow. The wetted area on the tubes is an issue that needs to be improved.
[84]	Horizontal tube bundle of 16 copper tubes with 122 mm OD	H_2O/LiBr	T_i (20 °C), X (55%), Γ (0.006–0.034 kg s^{-1} m^{-1})	It includes visual observation experiments. An optimum mass flow of 0.025 kg s^{-1} m^{-1} was obtained for tube wetting.
[85]	Plate desorber-rectifier containing microscale features	NH_3/H_2O	P (kPa), T_H (160–190 °C), T_w (50–125 °C), $\dot{m}$ (28.2–42.2 kg h^{-1}), $\dot{m}_H$ (0.067–0.101 kg s^{-1})	Desorption rate increased when the solution flow and heating temperature were increases.
[87]	Horizontal tube bundle of 80 copper tubes with 12 mm OD	H_2O/LiBr	P (4.4–5.5 kPa), T_H (65–85 °C), X (52–60%), Γ (0.004–0.026 kg s^{-1} m^{-1})	It includes visual oservation experiments. The solution mass flow improves the heat transfer because tube wettability is better.
[90,91]	Concentric helical tube generator with 20.9 cm OD. 4.05 m and 6.56 m for inner coil and outer coil length, respectively.	H_2O/LiBr	T_i (50 °C), X (55%), Γ (0.003–0.019 kg s^{-1} m^{-1})	It includes visual observation experiments. The heat transfer coefficient increased when mass flow and wetting efficiency were reduced. This brought about a more uniform film flow.
[88]	Compact plate-and-frame generator with structural copper fins.	H_2O/LiBr	P (5–20 kPa), T_i (70 °C), T_w-T_s (5–20 °C) X (50–60%), G (0.3–10 kg min^{-1} m^{-1})	Higher desorption rates than those achieved in previous studies.
[92]	Three channel plate generator. It included 120° of arc horizontal columns welded to the central channel	H_2O/LiBr	P (3.55–6.72 kPa), T_i (52.9–71.8 °C), T_H (58.2–83.8 °C), X (50.1–53.82%),$\dot{m}$ (0.026–0.028 kg s^{-1}), $\dot{m}_H$ (0.18–0.27 kg s^{-1}), $\dot{Q}$/A (7.72–39.1 kW m^{-2})	It includes visual observation experiments. The wettability of the plates improved with increasing the solution flow and heating flow temperature.
[93,94]	Plate desorber-rectifier containing microchannels and trays	NH_3/H_2O	P (1300–2600 kPa), X (37–52%), $\dot{m}$ (0.004–0.0115 kg s^{-1}), $\dot{m}_H$ (0.14 kg s^{-1}), $\dot{Q}$/A (5.7–17.5 kW m^{-2})	Solution heat transfer coefficients were as high as 3250 W m^{-2} K^{-1} and mass transfer coefficients as high as 0.0022 m s^{-1}.
[95]	Tube desorber with various trays and driven by flue gases.	NH_3/H_2O	P (1760 kPa), T_i (96 °C), X (42–52%), $\dot{m}$ (0.006 kg s^{-1})	Tube desorber driven by two passes of flue gases. Gases heat transfer coefficient up to 0.1 kW m^{-2} K^{-1}.
[96]	Two plate desorber-rectifier. A vertical column configuration and a branched tray configuration	NH_3/H_2O	$\dot{m}$ (0.0041–0.0067 kg s^{-1})	The branched tray concept provided a higher desorber heat load and refrigerant flow rate than the vertical column.
[97]	Shell with an internal helical coil. Effective area of 0.79 m^2. Shell made of steel. Nominal diameter of 254 mm and total height of 625.5 mm.	$NH_3/LiNO_3$	P (1200–1700 kPa), T_i (40–63 C), T_H (80–105 °C), X (51.9–55.3%),$\dot{m}$ (0.78–1.25 kg min^{-1}), $\dot{m}_H$ (14–21.5 kg min^{-1}), $\dot{Q}$/A (1.2–4.5 kW m^{-2})	Falling film boiling heat transfer coefficients up to 270 W m^{-2} K^{-1} and refrigerant vapour flow rates up to 0.11 kg s^{-1}.
[99]	Detachable falling film desorber with two entwined modules and a heat transfer area of 1.94 m^2	H_2O/LiBr	P (2.4–5.1 kPa), T_H (51.5–83.9 °C), X (46.8–54.9%), Γ (0.027–0.055 kg s^{-1} m^{-1}), V_H (0.029–0.084 m^3 h^{-1}), $\dot{Q}$/A (3.95–10.68 kW m^{-2})	Boiling heat transfer and mass transfer coefficients up to 0.64 kW m^{-2} K^{-1} and 7.8 × 10^{-5} m s^{-1}, respectively.
[98]	Two plate desorber-rectifier. A vertical column configuration and a branched tray configuration	NH_3/H_2O	P (1620–2840 kPa), T_H (170–190 °C), X (40–55%),$\dot{m}$ (0.7–1.3 g s^{-1}), $\dot{Q}$/A (kW m^{-2})	Desorber duty and solution heat transfer coefficients for the tray design were up to 0.8 kW and 11,900 W m^{-2} K^{-1}.

P (inlet solution pressure), X (solution concentration), Xs (inlet surfactant concentration), xv (mean vapour quality), T_i (inlet solution temperature), T_w (wall surface temperature), T_s (saturation temperature of the fluid), T_H (inlet heating fluid temperature), $\dot{m}$ (solution mass flow), Γ (solution mass flow per unit of length), G (solution mass flow per unit of area), G_H (heating fluid mass flow per unit of area), V (Solution volumetric flow), V_H (Heating fluid volumetric flow), $\dot{\mathbf{Q}}$ (heat transfer rate), $\dot{\mathbf{Q}}$/A (heat transfer rate per unit of area).

liquid/liquid heat exchange with a sensible heat rate varying from 10.1% to 52.6%. Regarding the total pressure drop, values ranged from 23 to 30 kPa and in zone one the pressure variation was negligible.

Wang et al. [109] tested the performance of a polyvinylidene fluoride (PVDF) membrane-based generator on LiBr/H_2O absorption refrigeration systems. The section tested consisted of a bundle of microporous hydrophobic membrane devices contained in a shell. This study showed that the desorption rate increased when the inlet solution temperature and the solution mass flux were increased. It was also observed that the desorption rate increased when solution pressure was reduced. The maximum desorption mass flux rate was around 2.2 kg m^{-2} hr^{-1}.

Táboas et al. [110] conducted a detailed study of NH_3/H_2O mixture boiling in a plate heat exchanger with three channels. In the desorber, the NH_3/H_2O mixture flowed upwards through the central channel while the heating water flowed downwards through the side channels. This study showed that NH_3/H_2O mixture boiling transfers improved when the solution mass flux and the heat flux were increased, reaching values as high as 20 kW m^{-2} K^{-1}. In

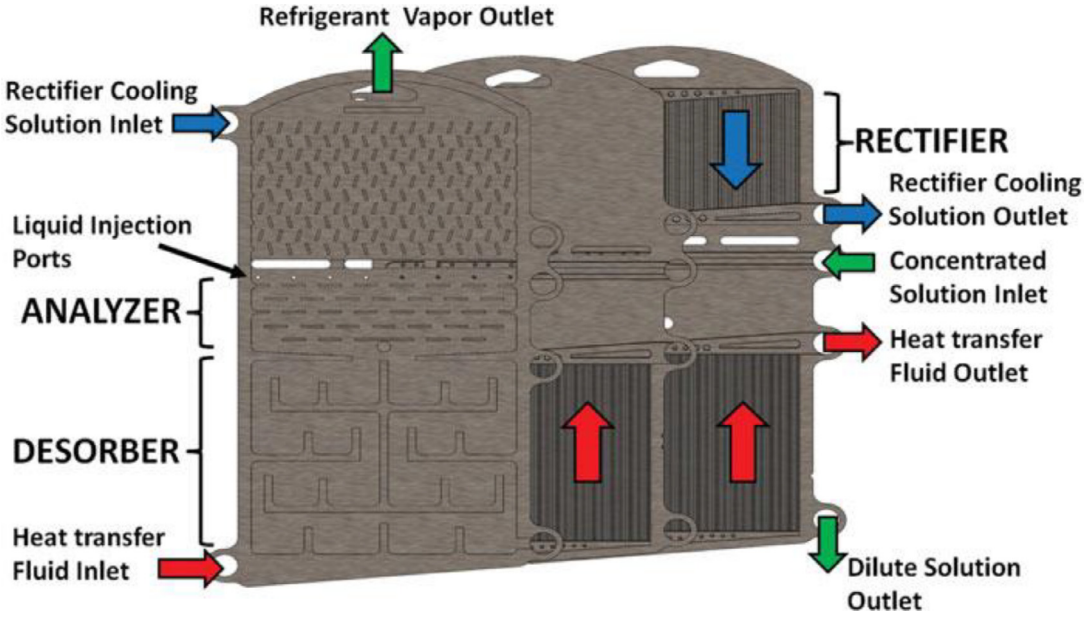

Fig. 8. Schematic design of the desorber-rectifier [85].

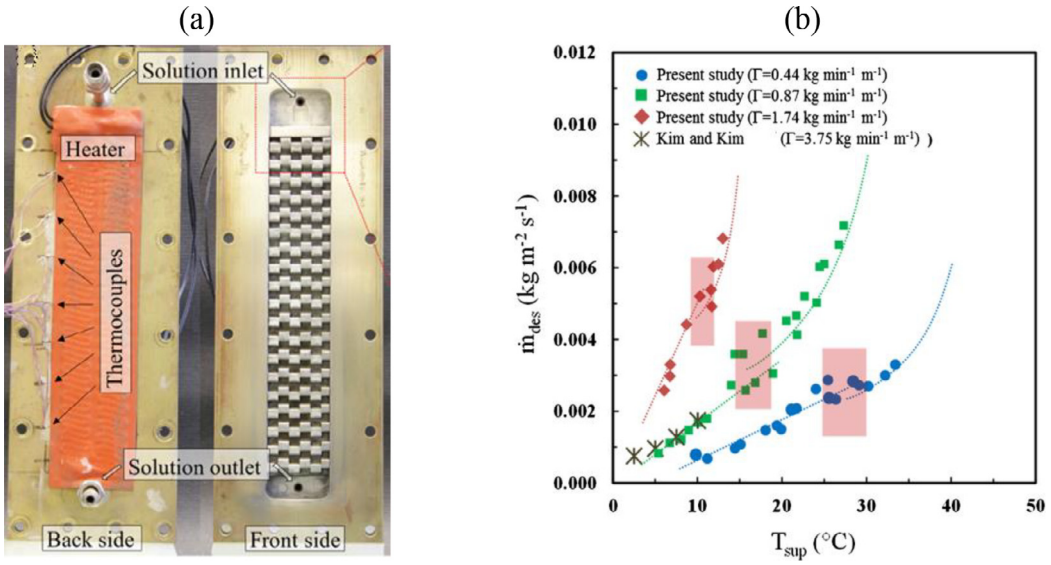

Fig. 9. (a) Compact generator concept, and (b) Desorption rate as a function of wall superheat and mass flux [88].

this case, the heat flux had a lesser impact on heat transfer than that of the mass flux. In the case of solution concentration and pressure, boiling heat transfer, at the studied conditions, was not noticeably affected. Furthermore, it was observed that heat transfer increased sharply when the solution approached saturation conditions, then it stayed steady until a mean vapour quality of 0.1 was reached. There the heat transfer increased again from this point on with mass fluxes above 100 kg m^{-2} s^{-1}. Pressure drop rose to 77 kPa when mass flux and mean vapour quality were increased, and system pressure was decreased.

Zacarías et al. [111] showed the boiling of a $NH_3/LiNO_3$ mixture in a 20 plate heat exchanger operating at the conditions of an absorption chiller. In the test section, the $NH_3/LiNO_3$ mixture flowed upwards while the heating water flowed downwards. The authors reported in Fig. 14 that the $NH_3/LiNO_3$ mixture boiling transfer increased up to values of 1.1 kW m^{-2} K^{-1} when solution mass flux and predominantly heat flux were increased. They also proposed a correlation for $NH_3/LiNO_3$ boiling heat transfer with an accuracy of within ±9% of error.

Balamurugan and Mani [112] evaluated a desorption process using R134a-Dimethyl formamide (DMF) as a working fluid in an absorption refrigeration test facility. The section tested in this study consisted of a double pipe heat exchanger where the solution flowed upwards, while the heating water flowed in a counter current. The authors found evidence that both the Sherwood and Nusselt numbers increased when the driving temperature, the R134a concentration, and the solution mass flow increased, and dropped when driving pressure was increased. Finally, the authors proposed dimensionless correlations for the Sherwood and Nusselt numbers with accuracies of within 15% and 25%, respectively. Further studies, this time on a plate heat exchanger, yielded similar observations to those made in the case of the double pipe heat exchanger [113]. In this study, they also reported correlations for the Sherwood and Nusselt numbers for the plate desorber. A comparison between the two heat exchangers with similar heat exchange areas showed that the compact heat exchanger outperformed the double pipe heat exchanger [114].

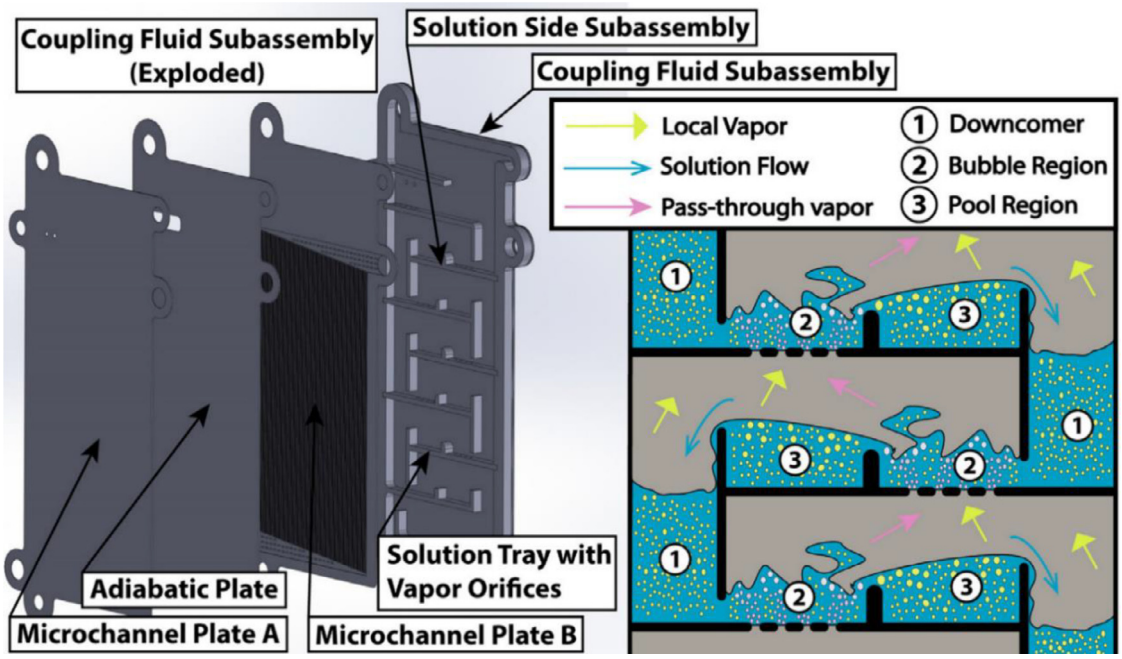

Fig. 10. Desorber-rectifier design concept, and flow pattern [93].

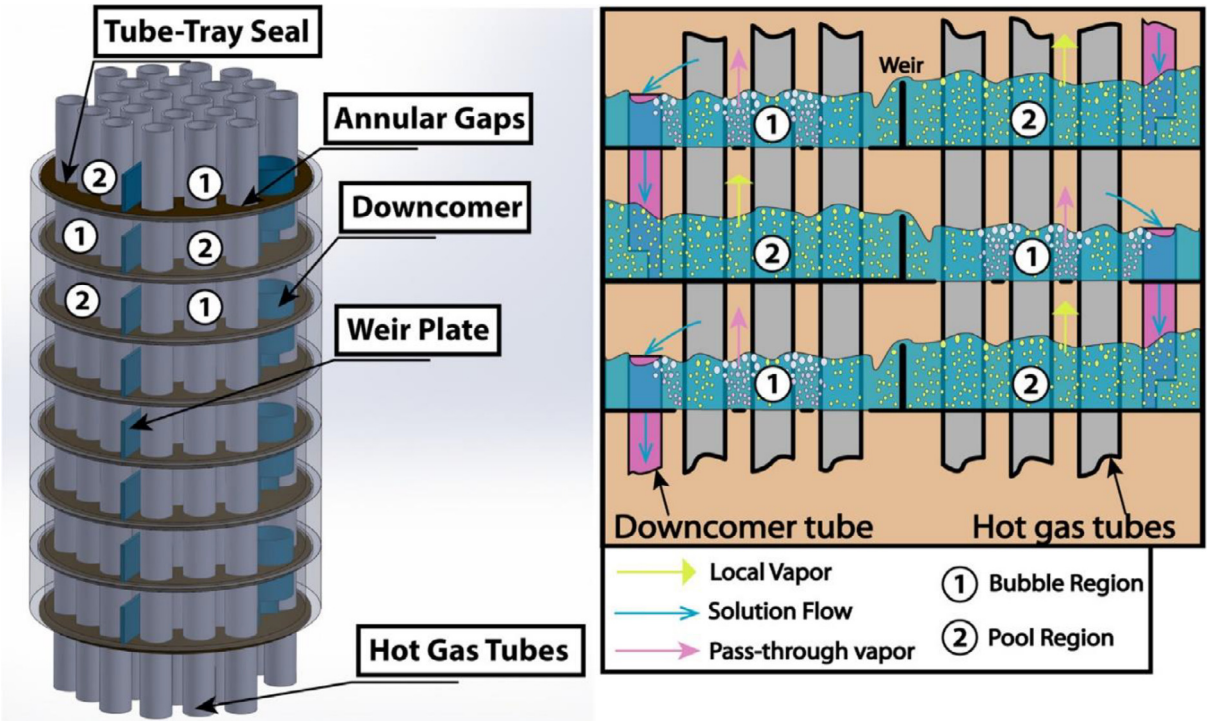

Fig. 11. Desorber design concept and flow pattern [95].

Venegas et al. [115] evaluated boiling heat transfer of a $NH_3/LiNO_3$ mixture in sub-cooled and saturated conditions in the same test facility used by Zacarías et al. [111]. This study pointed out that subcooled boiling reduced boiling heat transfer coefficients in line with those where subcooling was not contemplated. The authors also reported a boiling heat transfer correlation with an error of within 10%.

In a comparative study, Táboas et al. [116] used the data reported in [110] and evaluated the prediction for NH_3/H_2O mixture boiling heat transfer in plate heat exchangers from the correlations reported by Han et al. [117] and Donowski et al. [118]. Since those correlations tested failed to provide an acceptable prediction of boiling heat transfer data, the authors proposed a new correlation with an error of within 20%.

Following up on previous studies on membrane-based desorbers, Nasr Isfahani et al. [89,119] evaluated the use of membranes as absorbers and desorbers in an $H_2O/LiBr$ mixture absorption system test facility. In the case of the desorber, Fig. 15 shows the design used for these experiments. The membrane was 0.45 μm pore size whereas the desorber used a thin film as a heating

Fig. 12. Vertical column (left) and branched tray (right) test sections [98].

medium. In the study, the authors noted two boiling modes, i.e., direct diffusion, and nucleate boiling. During direct diffusion of water vapour, vapour pressure influenced desorption rate more than solution pressure did at the lowest wall temperature established, whereas solution pressure influenced desorption rate more significantly at the highest wall temperature. Also, higher desorption rates were obtained at low vapour and solution pressures due to lower saturation temperatures. Moreover, in the nucleate desorption mode, desorption rate increased when solution pressure was increased. As regards solution mass flow, its effect on the desorption rate was negligible. The authors concluded that the desorption rates obtained in their experiments were higher than those reported by Kim and Kim [79] and Thorud et al. [105]. In a study from the same research group, Bigham et al. [120] reported on the effect of a wall temperature on the desorption rate in a membrane desorber at different vapour and solution pressures. In this study, the authors indicated two desorption modes, a single-phase desorption mode and a two-phase mode. Results showed that by increasing the wall temperature, the desorption rate moved from single-phase to two-phase desorption, which is where desorption increases sharply, and nucleate boiling predominates. Moreover, the authors presented a numerical model of H_2O/LiBr mixture desorption using an in-house CFD solver, based on the Lattice Boltzmann Method (LBM). The objective of this study was to enhance desorption rates by inducing surface vortices by way of micro-ridges on the solution channels. Results showed that the use of micro-ridges increased desorption rate up to 1.7 times more than that of the base case.

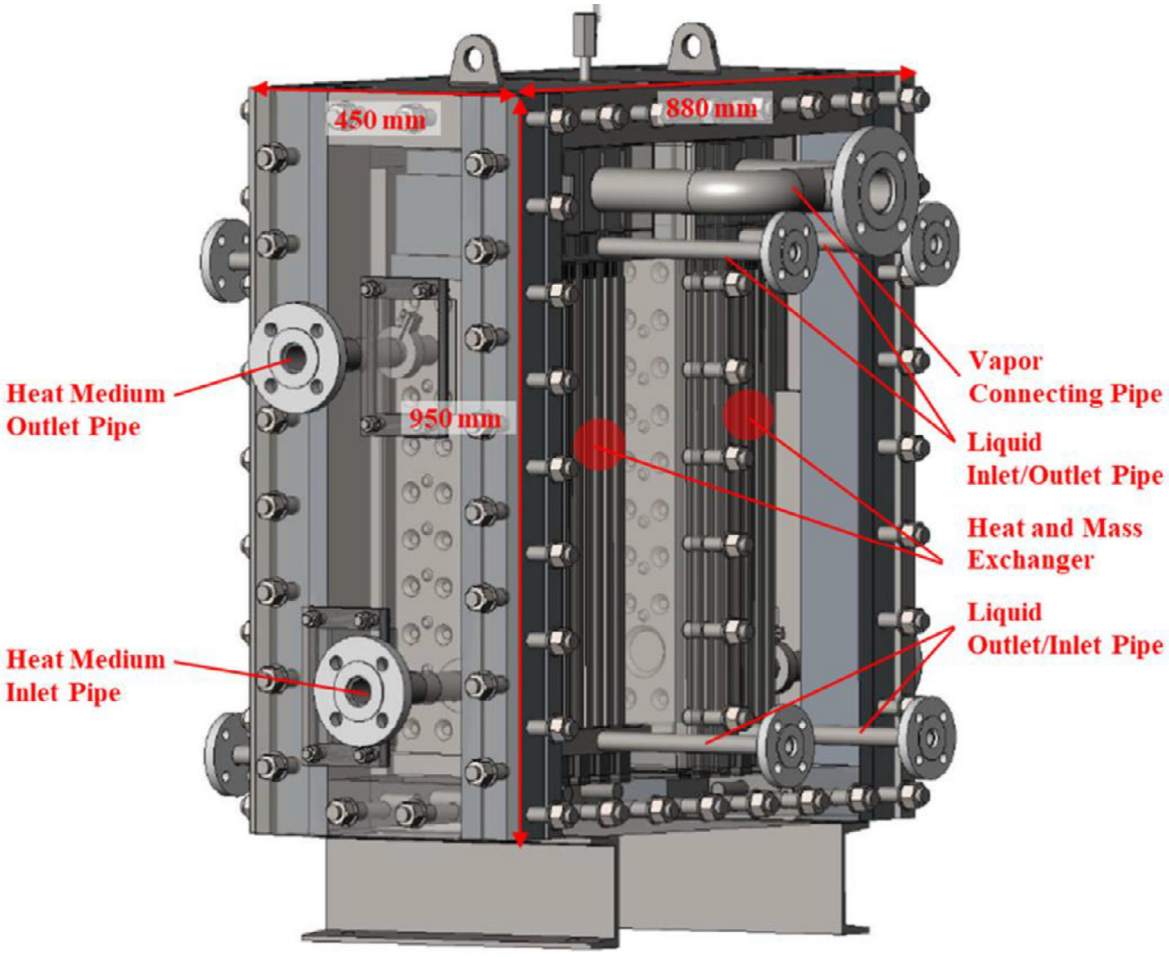

Fig. 13. Falling film generator proposed by [99].

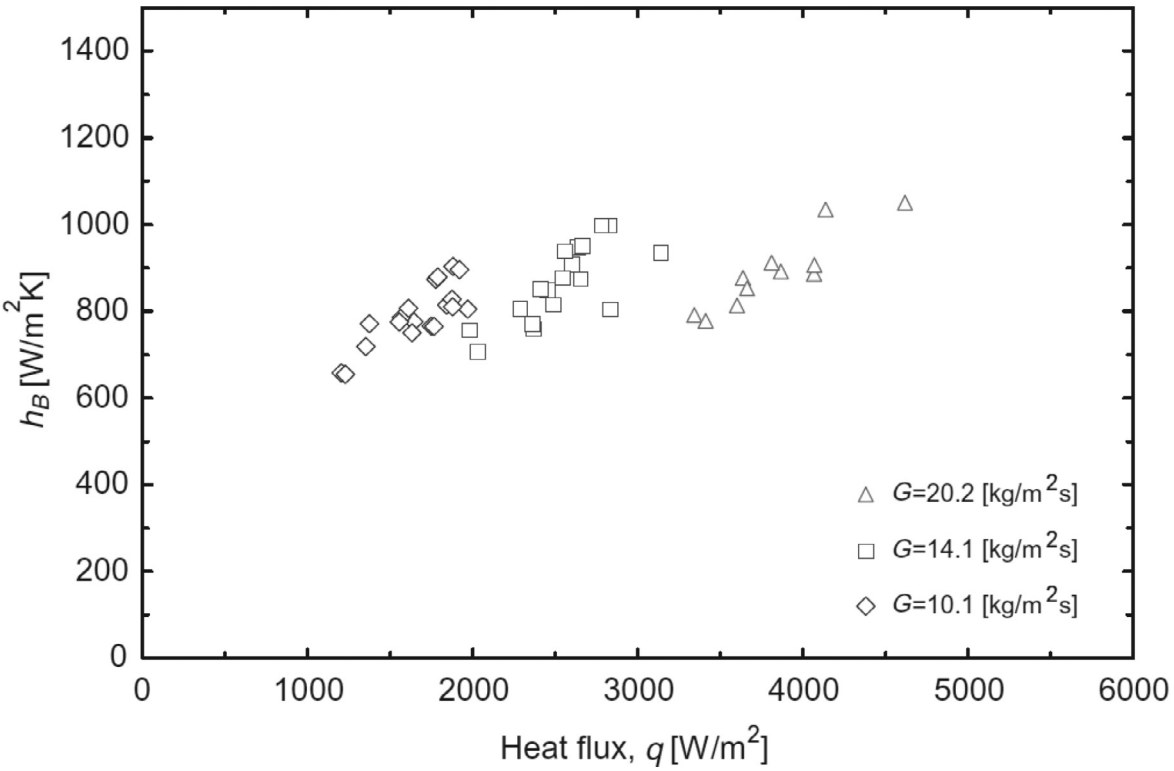

Fig. 14. Boiling heat transfer coefficient versus heat flux for various mass fluxes [111].

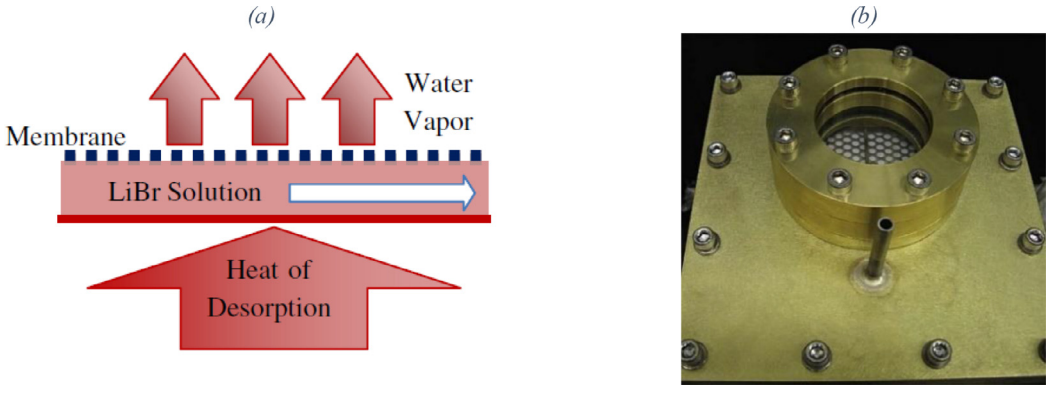

Fig. 15. (a) Schematic figure of a constrained solution flow in a membrane-based desorber and (b) the desorber [89].

Comparison between the boiling heat transfer of $NH_3/LiNO_3$ and $NH_3/(LiNO_3+H_2O)$ in a plate heat exchanger has also been reported [121–123]. These studies showed evidence that the boiling heat transfer for both mixtures increased when solution mass flux and heat flux were increased. However, the effect of the heat flux on the boiling heat transfer was less pronounced at low mass fluxes and with the highest vapour quality established. This means that both convective (low heat fluxes and high solution mass flow) and nucleate boiling (high heat fluxes and low solution mass flow) occurred in these experiments. Results also showed that boiling heat transfer for the ternary mixture was higher than that of the binary mixture because of its lower viscosity and higher thermal conductivity. Táboas et al. [122] also presented the pressure drop in the plate heat exchanger for both mixtures. Those results evidenced a lower pressure drop for the ternary mixture compared to that of the binary mixture. Finally, Táboas et al. [122] evidenced that the correlations proposed in [116] adequately reproduce the experimental data for both mixtures within errors of 20%.

Jiang et al. [124] presented the flow boiling of a $NH_3/LiNO_3$ mixture in a horizontal double pipe desorber which used water as a heating medium. This study evidenced the effect of mass flux, heat flux, and vapour quality on a boiling heat transfer. Results in Fig. 16 evidenced that effect of solution mass flux on the boiling heat transfer coefficient was more evident at heat fluxes below 20 kW m^{-2} than at those above 20 kW m^{-2}. Moreover, the boiling heat transfer coefficients increased when heat flux was increased up to 1950 W m^{-2} K^{-1}. This indicates that the nucleate boiling mechanism seems to influence these experiments. It was also observed that higher exit vapour quality values are obtained at heat fluxes below 20 kW m^{-2} while they decrease when solution mass flux increases. Finally, the authors pointed out that the experimental data had been appropriately predicted by the correlation in [28].

Further studies carried out in the same test facility showed the effect of inner tube diameter on boiling heat transfer [125]. The authors showed that the boiling heat transfer coefficient decreased when the inner tube diameter was reduced from 6 mm to 4 mm

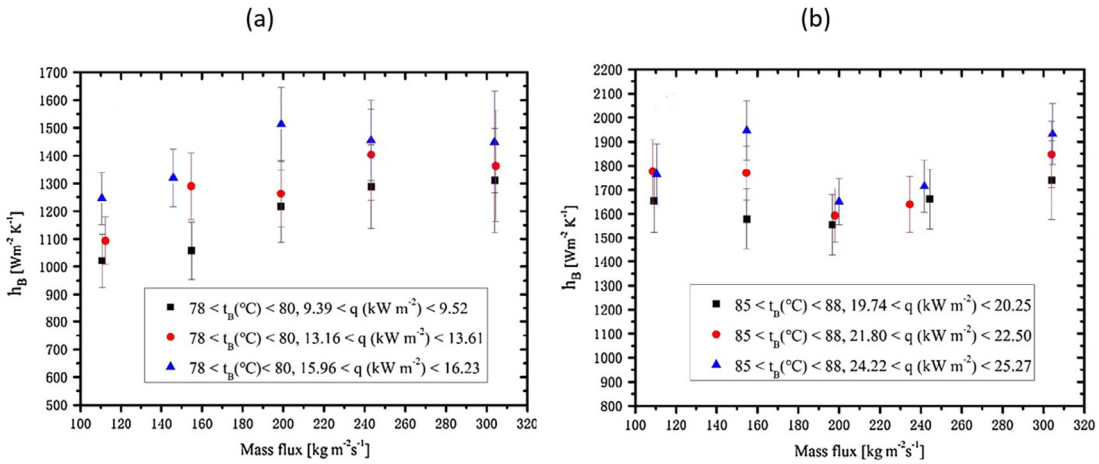

Fig. 16. Mass flux versus boiling heat transfer coefficient and temperature range (a) 78–80 °C; (b) 85–88 °C [124].

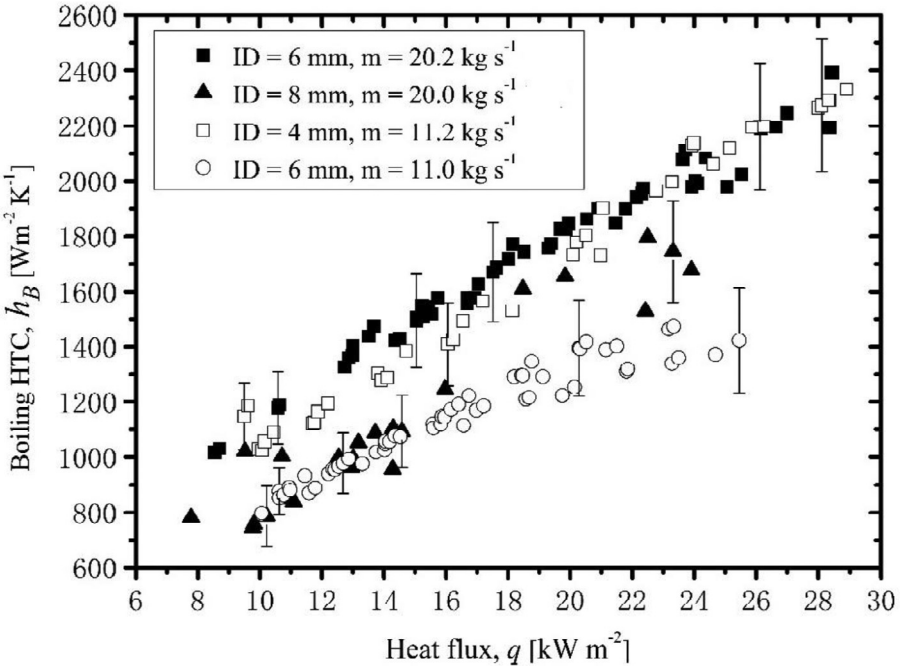

Fig. 17. Flow boiling heat transfer versus heat flux, mass flow rates, and three inner tube diameters [125].

for all test conditions. Moreover, comparison with previous results using a tube with an inner diameter of 8 mm evidenced that the boiling heat transfer in a 8 mm ID tube was higher than that of other tubes of smaller diameters when solution mass flux was below 155 kg m^{-2} s^{-1} and for all the range of heat fluxes [124]. As shown in Fig. 17, for higher mass fluxes, boiling heat transfer in an 8 mm ID tube dropped below the values in data reported for other tubes. The authors proved that at a solution mass flux below 155 kg m^{-2} s^{-1}, the contact area between the liquid and the tube wall decreases when the tube diameter is decreased. This could result in a reduction in convective heat transfer and mass diffusion. Moreover, mass diffusing resistance in smaller tubes decreases when solution mass flux is increased to above 155 kg m^{-2} s^{-1}. Results indicated that the selection of an optimum tube diameter is a key parameter in the design of desorbers. To conclude this study, the authors reported a boiling heat transfer correlation that predicts the experimental data to within errors of 20%.

Ibarra-Bahena et al. [126] tested a membrane-based desorber/condenser for LiBr/H_2O absorption systems. The section tested consisted mainly of two walls, a hydrophobic membrane, and a cooling plate. In this desorber/condenser, the solution flowed upwards through the desorber/condenser while the refrigerant vapour passed through the membrane. The vapour coming through the membrane was condensed on coming into contact with the cooling plate (see Fig. 18). This study showed that the desorption rate increased when solution temperature and solution flow were increased. It was also observed that the effect of solution mass flow was more pronounced when solution temperature was increased and solution concentration was reduced. Maximum desorption rate reached 9.8 kg m^{-2} h^{-1}. Meanwhile, Hong et al. [127] evaluated the performance of a hydrophobic polypropylene membrane-based generator with a LiBr/H_2O mixture (see Fig. 19) in the same test facility used in [109]. In addition to the previous outputs reported in [109], it was observed that desorption rate increased when the inlet solution concentration was reduced. The maximum desorption mass flux rate was around 4.9 kg m^{-2} hr^{-1}.

Cai et al. [128] reported a NH_3/NaSCN mixture boiling heat transfer in the same test section used in [125]. This study showed

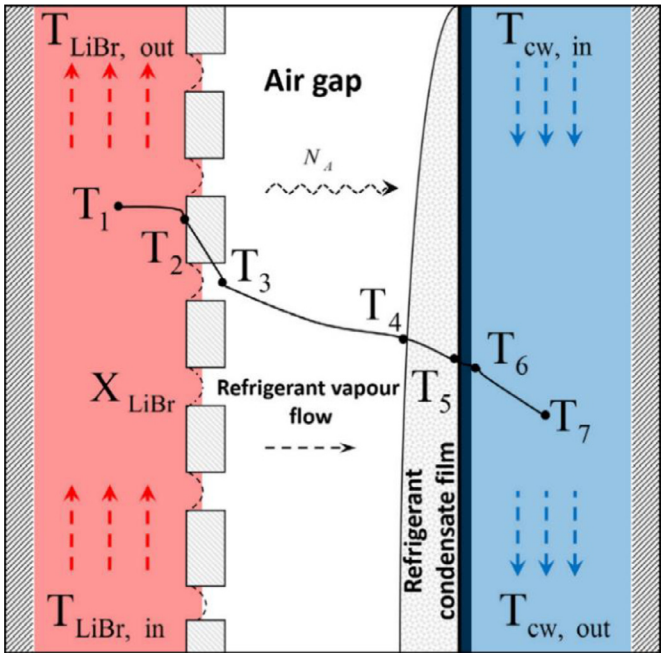

Fig. 18. Diagram of the desorption-condensation process [126].

that the boiling heat transfer coefficient for the NH_3/NaSCN mixture was higher than that of the NH_3/$LiNO_3$ mixture at similar test conditions. This was due to the lower viscosity and the higher thermal conductivity of the working fluid (see Fig. 20).

Venegas et al. [129] used a membrane-based desorber with a 0.45 μm pore diameter to study a LiBr/H_2O mixture desorption process (see Fig. 21). They reported on the effect of solution flow and heating water temperature on desorption rates. Desorption rates of up to 4.2 kg m^{-2} s^{-1} were included in the report with the highest solution flows and heating water temperatures established.

Ibarra-Bahena et al. [130] tested a membrane desorber in a LiBr/H_2O mixture absorption cooling system by varying the inlet solution temperature. In this case, the desorber used a hydrophobic membrane with a 0.22 μm pore diameter. The desorption rates reported in this study were up to 5.7 kg m^{-2} h^{-1} at an inlet solution temperature of 95.2 °C.

Li et al. [131] and Zhou et al. [132] continued the research conducted by Jiang et al. [125] and Cai et al. [128] on a horizontal double pipe desorber, but this time the working fluids were R290/mineral-oil and R290/POE-oil. Zhou et al. [132] showed that both convective and nucleate boiling were responsible for the flow boiling heat transfer at the different operating conditions set as the transfer increased when solution mass flux and heat flux were increased. As in previous experiments with other fluids, smaller tube diameters also improved boiling heat transfer. Moreover, boiling heat transfer reached 800 W m^{-2} K^{-1} and was obtained at the highest heat flux and mass flux set for the experiments. In the case of the results reported by Li et al. [131], neither nucleate boiling nor convective boiling were found to be dominant in the R290/mineral-oil mixture boiling heat transfer. It is important to highlight that the results reported in these studies are significantly lower than those obtained from the NH_3/$LiNO_3$ and NH_3/NaSCN mixtures in the same test section [125,128].

To conclude this sub-section, it is worth mentioning that most of the studies on forced flow boiling, found in the literature, deal with the characterization of the boiling process in different desorber configurations with a special interest in compact designs such as membrane and plate desorbers. Moreover, various studies have identified and discussed the contribution of diffusion, convective, and nucleate boiling to boiling processes. No studies have

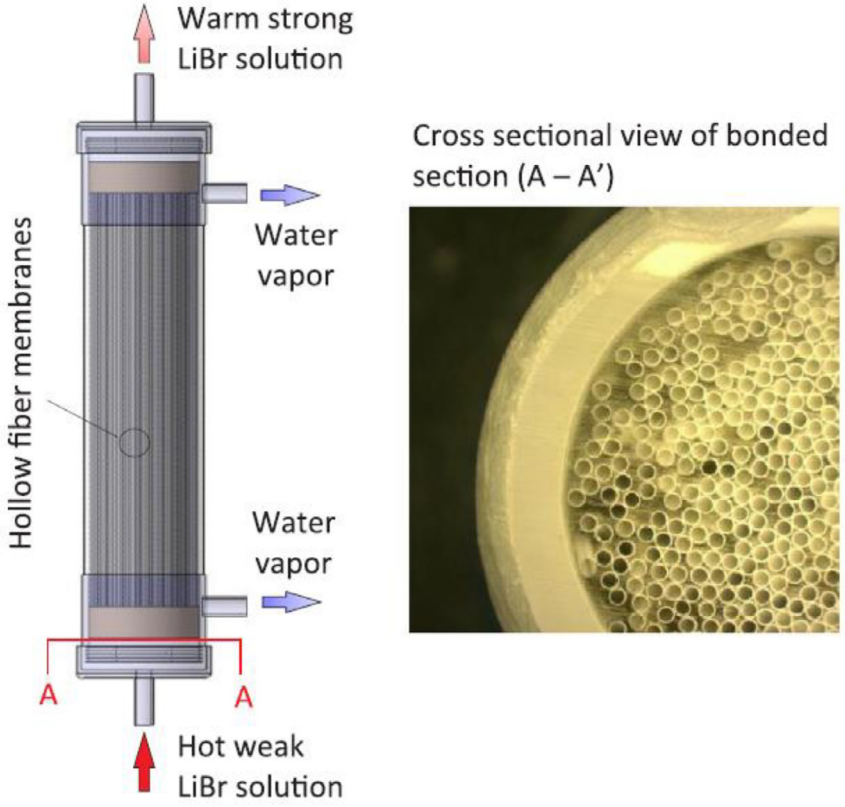

Fig. 19. membrane-based desorber [127].

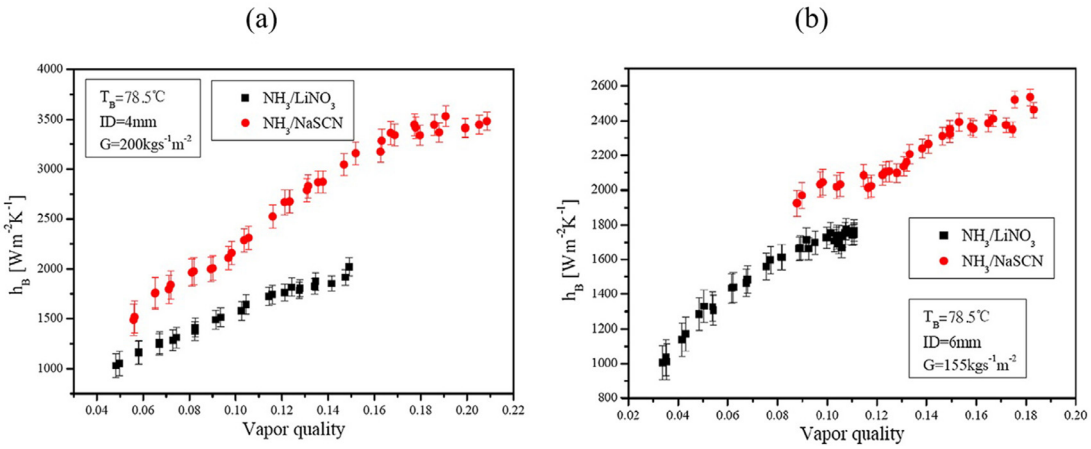

Fig. 20. Flow boiling heat transfer coefficients of NH_3/NaSCN and NH_3/LiNO3:versus vapour quality (a): tube ID=4 mm, G = 200 kg/(m2 s); (b): tube ID=6 mm, G = 155 kg/(m2 s) [128].

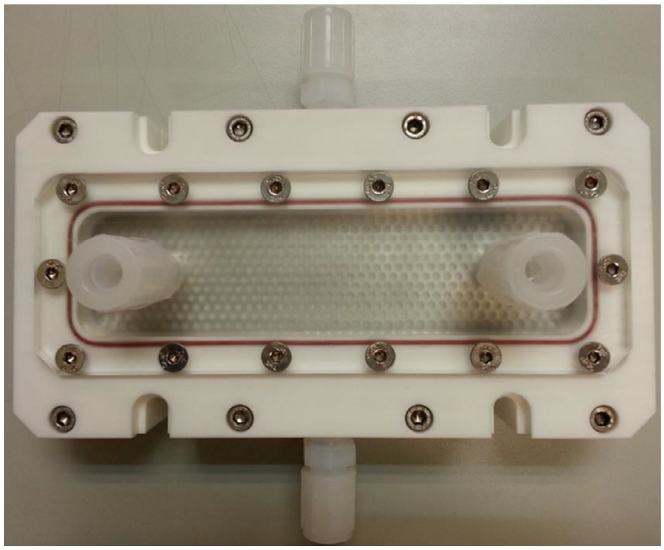

Fig. 21. membrane-based desorber [129].

been found using additives or nanofluids to enhance heat and mass transfer processes in desorbers. As concluded by Cheng et al. [133], boiling studies involving surfactants or nanoparticles to enhance boiling processes in desorbers are still at an early stage of development.

The present review also shows that the number of studies, reported in the literature, on boiling processes in desorbers for absorption heat pump technologies is significantly lower than the number of studies dealing with the characterization of the absorption process and its enhancement [17]. This evidences the potential for research into boiling characterization features and intensification by means of additives and nanofluids to develop more compact absorption systems. Table 3 provides a compendium of the experimental studies on flow boiling conditions using conventional and promising working fluids for absorption heat pumps.

3.4. Heat and mass transfer correlations

This section is devoted to the review of heat and mass transfer correlations, reported from studies carried out on the boiling process, using working fluids specifically for absorption heat pumps.

Various correlations have been reported to predict the boiling of pure fluids and mixtures. In the case of pure fluids such as ammonia or water, correlations available in the literature have been found to predict pool boiling heat transfer reasonably well [19,66]. For binary mixtures like those used in absorption heat pumps, the general correlations reported can be found in [41–43,45,71,72,134,135], However, these correlations require adjustments to be made to the parameters before other researchers can use them to predict boiling heat transfer for absorption heat pumps satisfactorily, using other working fluids, in different configurations, and at other operating conditions.

More specific correlations for heat and mass transfer in absorption heat pumps are also available in the literature and have been obtained from tests on desorbers using proper working fluids. Investigations dealing with the development of those correlations are summarised in Table 4. The table includes the reference to the correlations, correlated parameter, working fluids used, desorber type, and the corresponding accuracies.

Table 4 shows that the first correlations were obtained mainly from tests on pool desorbers, then the focus moved to the development of correlations for forced flow and falling-film desorber configurations. It is worth note that most of the correlations were obtained using NH_3/H_2O mixtures, followed by $NH_3/LiNO_3$ mixtures, and only a couple of correlations were reported using H_2O/LiBr or R134A-DMF mixtures.

Regarding the correlations reported for pool boiling, Charters et al. [62] based their correlation on the Nusselt number and the Stanton number. From the correlations reported by Inoue et al. [135] and Stephan and Korner [72], Arima et al. [65] based their correlation on the ideal heat transfer coefficient together with a correction factor which contemplated the temperature difference between dew and boiling point, and the mole fraction of liquid and vapour. Táboas et al. [66] combined the correlations reported by Schlunder [41] and Thome and Shakir [42] to propose a fitted correlation to predict pool boiling at low and high ammonia concentrations. Meanwhile, Inoue and Monde [67] observed that nucleate boiling occurring with a NH_3/H_2O mixture was mainly controlled by the mole fraction of liquid and vapour and consequently updated the correlation reported previously in [135]. Similarly, Sathyabhama and Ashok Babu [69] proposed a adapted correlation based on those correlations reported by Calus and Rice [71] and Stephan and Korner [72].

As regards the correlations reported for falling-film desorbers, Shi et al. [81,82] based their correlation on solution concentration, heat flux, and the Reynold number, including fitting regression parameters. Staedter and Garimella [94] considered the ideal pool boiling correlations as those used by Thome and Shakir [42] and Fujita and Tsutsui [134] and added a fitted correction parame-

Table 3
Compendium of the experimental studies on forced flow boiling desorbers for absorption heat pumps.

Reference	Test section	Working fluids	Test condition ranges	Note
[100]	Vertical cylinder heated by a gas burner	H_2O/LiBr	X (56%), $\dot{Q}$ (11.7–21.2 kW)	Refrigerant desorbed increased linearly with heat input.
[101]	Vertical stainless-steel tube of 31.8 mm OD and wall thickness of 3.0 mm.	NH_3/H_2O and $NH_3/LiNO_3$	P (870–1480 kPa), X (39–48%), G (4.2–13.7 kg m^{-2} s^{-1}), $\dot{Q}/A$ (11.2–18.1 kW m^{-2})	Proposal of Correlations. Heat transfer with NH_3/H_2O higher than that with $NH_3/LiNO_3$.
[102]	Membrane-based desorber/condenser	H_2O/(Potassium formate+caesium formate)	P (2.2–4.2 kPa), T_i (70 °C), X (55–78%),), Xcaesium (25%), V (0.1–3.5 L min^{-1})	Desorption rate increases when solution pressure and concentration are reduced. Desorption rate significantly improves by adding caesium formate to the base mixture.
[103,104]	Stainless steel vertical double pipe. Internal tube of 6/9 mm ID/OD. External tube of 28/32 mm ID/OD. Water heated length of 1 m.	NH_3/H_2O	P (150–2000 kPa), T_i (40 °C), T_s (70–90 °C), X (42–61%),G (707–2688 kg m^{-2} s^{-1}), $\dot{Q}/A$ (8.211–18.521 kW m^{-2})	Effect of $\dot{Q}/A$ and G on NH_3/H_2O boiling found to be greater than that of the X.
[105]	Membrane-based desorber of 2.9 cm wide and 5.8 cm long	H_2O/LiBr	P (33.5 kPa), X (32–50%), $\dot{m}$ (0.0032 kg h^{-1})	Desorption rate improves as the wall superheating increases and as the LiBr mass fraction decreases.
[106]	Plate heat exchanger with a heat transfer area of 0.53 m^2. Thermal oil used as a heating medium.	H_2O/LiBr	P (130 kPa), T_s (128.5–141.5 °C), T_H (187.2–196.5 °C), X (56%), G (40.3–112 kg m^{-2} s^{-1}), G_H (360 kg m^{-2} s^{-1}), $\dot{Q}$ (23.4–26.5 kW)	Tests in an actual absorption machine. Prototype. Refrigerant vapour quality during boiling between 2% and 6%. Boiling heat transfer up to 5.2 kW m^{-2} K^{-1}.
[109]	Bundle of PVDF microporous hydrophobic membrane devices with porosity of 85% in a shell	H_2O/LiBr	P (5–15 kPa), T_i (65–88 °C), X (50%), G (40–120 kg m^{-2} s^{-1})	Desorption mass flux rate up to 2.2 kg m^{-2} hr^{-1}.
[110]	Stainless steel plate heat exchanger with a heat transfer area of 0.1 m^2. Water used as a heating medium.	NH_3/H_2O	P (700–1500 kPa), X (42–62%),vx (0–20%), G (50–140 kg m^{-2} s^{-1}), $\dot{Q}/A$ (20–50 kW m^{-2})	Effect of G and vapour quality on the boiling heat transfer found greater than that of and $\dot{Q}/A$. Effect of X and P on boiling found to be slight.
[111]	Stainless steel plate heat exchanger with a heat transfer area of 1.8 m^2. Water used as a heating medium.	$NH_3/LiNO_3$	P (977.7–1606 kPa), T_s (72.8–90.1 °C), X (45.2–46.2%), T_w-T_s (1.3–2.8 °C), G (10.0–20.2 kg m^{-2} s^{-1}), G_H (44.8–46.8 kg m^{-2} s^{-1}), $\dot{Q}/A$ (1203–4618 kW m^{-2})	Boiling heat transfer increased by increasing G and $\dot{Q}/A$. Proposal of Correlation.
[112]	Stainless steel double pipe. Inside tube with 20/23 mm ID/OD, outside tube with 30/33 mm ID/OD. Tube length of 1000 mm. Water used as a heating medium.	R134a/DMF	P (650–1000 kPa), T_s (78–90 °C), T_H (82–98 °C), X (58–76%), V (0.02–0.05 m^3 hr^{-1}), V_H (0.08–0.33 m^3 hr^{-1})	Proposal of correlations.
[113]	Stainless steel plate heat exchanger with a heat exchange area of 0.16 m^2. Water used as a heating medium.	R134a/DMF	P (620–920 kPa), T_s (80–95 °C), X (59–75%), V (0.02–0.05 m^3 hr^{-1}), V_H (0.12–0.32 m^3 hr^{-1})	Proposal of correlations.
[115]	Stainless steel plate heat exchanger with a heat exchange area of 1.8 m^2. Water used as a heating medium.	$NH_3/LiNO_3$	P (980–1610 kPa), T_s (72.8–90.1 °C), X (45.2–46.2%), G (9.9–19.8 kg m^{-2} s^{-1}), G_H (44.1–46.1 kg m^{-2} s^{-1})	Subcooled boiling reduced the boiling heat transfer coefficients. Proposal of correlations.
[89,119]	Membrane-based desorber with an overall size of 16.8 × 16.5 cm^2 and a 5.7 × 8.9 cm^2 area. Membrane of 0.45 µm	H_2O/LiBr	P (13–30 kPa, T_i (50–70 °C), T_w (50–125 °C), X (50%), $\dot{m}$ (0.75–3.25 kg h^{-1})	Vapour pressure was predominant on direct diffusion whereas the solution pressure was predominant on boiling desorption.
[122]	Stainless steel plate heat exchanger with a heat transfer area of 0.1 m^2. Water used as a heating medium.	$NH_3/LiNO_3$ and $NH_3/(LiNO_3+H_2O)$	P (1200–1500 kPa), X (49–54%), Xternary (42–46%), X_{H2O} (20%), vx (0–16%), G (50–100 kg m^{-2} s^{-1}), $\dot{Q}/A$ (20–50 kW m^{-2})	Boiling heat transfer for the ternary mixture was higher than that of the binary mixture.
[124]	Stainless smooth horizontal double pipe with the inner tube of 8/10 mm ID/OD, the outer tube of 14/16 ID/OD, and length of 1.1 m	$NH_3/LiNO_3$	P (992.3–1531.9 kPa), T_s (76.7–93.2 °C), X (45.5%), G (110–304 kg m^{-2} s^{-1}), V_H (0.054–0.253 m^3 h^{-1}), $\dot{Q}/A$ (7.8–34.5 kW m^{-2})	The effect of the heat flux on boiling heat transfer was more dominant than that of the mass flux.
[125]	Stainless smooth horizontal double pipe with the outer tube of 15/16 ID/OD, length of 1.1 m, and various inner tube diameters	$NH_3/LiNO_3$	P (1030.2–1457.6 kPa), T_s (78–90 °C), X (45.5%), G (110–304 kg m^{-2} s^{-1}), V_H (0.054–0.253 m^3 h^{-1}), $\dot{Q}/A$ (7.72–39.1 kW m^{-2}), Inner tube inner diameter (4, 6 mm)	Smaller inner tubes increase boiling heat transfer at high mass fluxes. Boiling heat transfer up to 2650 W m^{-2} K^{-1}.
[126]	Hydrophobic membrane-based desorber/condenser with 0.45 µm pore size	H_2O/LiBr	T_i (74.4–95.9 °C), X (45.68–58.66%), $\dot{m}$ (0.0154–0.0245 kg s^{-1})	Desorption rate up to 9.8 kg m^{-2} h^{-1}.
[127]	Bundle of polypropylene microporous hydrophobic membrane devices with porosity of 50% in a shell	H_2O/LiBr	P (2.5–5.5 kPa), T_i (65–83 °C), X (51–58%), G (157–244 kg m^{-2} s^{-1})	Desorption mass flux rate up to 4.9 kg m^{-2} hr^{-1}.
[128]	Stainless smooth horizontal double pipe with the outer tube of 15/16 ID/OD, length of 1.1 m, and various inner tube diameters	NH_3/NaSCN	P (1108–1497 kPa), T_s (78–91 °C), X (42.9–44.5%), G (110–304 kg m^{-2} s^{-1}), V_H (0.054–0.253 m^3 h^{-1}), $\dot{Q}/A$ (10.27–42.9 kW m^{-2}), Inner tube inner diameter (4, 6,8 mm)	Boiling heat transfer coefficients for the NH_3/NaSCN mixture higher than those of the $NH_3/LiNO_3$.

(*continued on next page*)

Table 3 (*continued*)

Reference	Test section	Working fluids	Test condition ranges	Note
[131]	Stainless smooth horizontal double pipe with a length of 1.1 m, and various inner/outer tube diameters	R290/mineral oil	P (920–1120 kPa), T_s (59–71 °C), X (15%), G (221–387 kg m^{-2} s^{-1}), V_H (0.059–0.123 m^3 h^{-1}), $\dot{Q}$/A (14–27 kW m^{-2}), Inner tube inner diameter (4,6,8 mm), outer tube inner diameter (10,12,14 mm)	Neither the nucleate boiling mechanism nor convective boiling mechanism were found dominant. Boiling heat transfer up to 1600 W m^{-2} K^{-1}.
[129]	Membrane-based microchannel desorber with mass transfer area around 4.28 m^2	H_2O/LiBr	T_i (28 °C), T_H (62–66 °C), X (45.8%), $\dot{m}$ (0.5–1.7 kg h^{-1}), V_H (0.2 L min^{-1})	Desorption rates up to 4.2 kg m^{-2} s^{-1}.
[130]	Membrane-based microchannel desorber with mass transfer area around 1 m^2	H_2O/LiBr	T_i (75.3–95.2 °C), X (49.78%), $\dot{m}$ (0.025 kg s^{-1}), V_H (2.0 L min^{-1})	Desorption rates up to 5.7 kg m^{-2} h^{-1}.
[132]	Stainless smooth horizontal double pipe with a length of 1.1 m, and various inner/outer tube diameters	R290/POE-oil	P (1200–1400 kPa), T_s (55.3–62.5 °C), X (11.1%), G (166–387 kg m^{-2} s^{-1}), V_H (0.029–0.084 m^3 h^{-1}), $\dot{Q}$/A (1.0–30.74 kW m^{-2}), Inner tube inner diameter (4,6,8 mm), outer tube inner diameter (10,12,14 mm)	Boiling heat transfer up to 800 W m^{-2} K^{-1}.

P (inlet solution pressure), X (solution concentration), Xs (inlet surfactant concentration), xv (mean vapour quality), T_i (inlet solution temperature), T_w (wall surface temperature), T_s (saturation temperature of the fluid), T_H (inlet heating fluid temperature), $\dot{m}$ (solution mass flow), Γ (solution mass flow per unit of length), G (solution mass flow per unit of area), G_H (heating fluid mass flow per unit of area), V (Solution volumetric flow), V_H (Heating fluid volumetric flow), $\dot{\boldsymbol{Q}}$ (heat transfer rate), $\dot{\boldsymbol{Q}}$/A (heat transfer rate per unit of area).

Table 4
Summary of the available heat and mass transfer correlations using various working fluids in desorbers for absorption heat pump systems.

Reference	Working fluids	Correlated parameter	Desorber type/ solution flow configuration	Accuracy range
[62]	H_2O/LiBr	Boiling heat transfer coefficient	Vessel/ Pool flow	–
[101]	NH_3/H_2O and $NH_3/LiNO_3$	Boiling heat transfer coefficient	Vertical tube/ Forced upward flow	±25%
[65]	NH_3/H_2O	Boiling heat transfer coefficient	Vessel/ Pool flow	–
[66]	NH_3/H_2O	Boiling heat transfer coefficient	Vessel/ Pool flow	±40%
[67]	NH_3/H_2O	Boiling heat transfer coefficient	Vessel/ Pool flow	±20%
[81,82]	H_2O/LiBr	Boiling heat transfer coefficient	Vertical tube/ Falling film flow	19%
[111]	$NH_3/LiNO_3$	Nusselt number	Vertical plate heat exchanger/ Upward flow	±9%
[69]	NH_3/H_2O	Boiling heat transfer coefficient	Vessel/ Pool flow	±18%
[112]	R134a-DMF	Nusselt and Sherwood numbers	Vertical double pipe/ Forced upward flow	±25% and ±15%, respectively.
[113]	R134a-DMF	Nusselt and Sherwood numbers	Vertical plate heat exchanger/ Forced upward flow	±25% and ±15%, respectively.
[115]	$NH_3/LiNO_3$	Nusselt number	Vertical plate heat exchanger/ Forced upward flow	±10%
[116]	NH_3/H_2O	Boiling heat transfer coefficient	Vertical plate heat exchanger/ Forced upward flow	±20%
[125]	$NH_3/LiNO_3$	Boiling heat transfer coefficient	Horizontal double pipe/ Horizontal flow	±20%
[94]	NH_3/H_2O	Boiling heat transfer coefficient	Plate desorber-rectifier/ Falling film flow	±25%
[97]	$NH_3/LiNO_3$	Nusselt number	Shell with an internal helical coil/ Falling film flow	±20%
[98]	NH_3/H_2O	Boiling heat transfer coefficient	Branched tray configuration/ Falling film flow	±25%

ter for the binary mixture based on that reported by Mostinski [25]. Hernández-Magallanes and Rivera [97] reported a Nusselt correlation based on the Prandtl, Boiling, Jacob, and Froude numbers. Meanwhile, Delahanty et al. [98] based their correlation on the ideal phase-change heat transfer coefficient, the vapour-to-interface heat transfer coefficients, and the ratio of vapour sensible heat flow to total heat flow.

Regarding the correlations reported for forced flow desorbers, Rivera and Best [101] used the Lockhart and Martinelli parameter (X_{tt}).and the Boiling number (B_o) for the development of their correlations. Zacarías et al. [111] and Venegas et al. [115] based their correlation on the Prandtl, Boiling, Jacob and Froude numbers. Balamurugan and Mani [112] correlated the Nusselt number with the two-phase Reynold number, Lockhart and Martinelli parameter, and the Boiling number, whereas Balamurugan and Mani [113] considered only the Reynold number and the Prandtl number. Moreover, the Sherwood number for mass transfer in each study was correlated using the two-phase Reynold number, momentum diffusivity, heat flux, and concentration difference between the solution inlet and outlet. Táboas et al. [116] developed their correlations for both convective boiling and nucleate boiling where the deciding factor was the superficial velocity of vapour. If nucleate boiling is predominant, the effect of the Boiling number and single-phase heat transfer coefficient is considered. If convective boiling occurs, then the effect of the Lockhart and Martinelli parameter and the single-phase heat transfer coefficient are associated. Also, Jiang et al. [125] reported a boiling heat transfer correlation considering both, convective boiling and nucleate boiling, with their respective suppression factors. The suppression factor for convective boiling includes the Lockhart and Martinelli parameter, the Boiling number, and the Weber number, whereas the Reynolds number and tube diameter were taken into consideration in the case of nucleate boiling.

From the revision conducted, it can be concluded that there is still much work to do to develop proper correlations to characterise boiling heat transfer in compact desorbers for absorption heat pumps. Most of the correlations were obtained from experiments in vessels, vertical tubes, or plate desorbers. The correlations reported are all different in form and parameters considered, plus they were obtained under specific operating conditions. Therefore, they should be tested to know how they reproduce the data reported by other researchers. Moreover, in forced flow boiling, only a couple of correlations contemplate convective and nucleate modes [116,125]. In the other correlations, only one effect was found to be predominant according to the experimental operating conditions and results.

4. Conclusions and future works

The present review was aimed at facilitating the evolution of investigations dealing with the characterization of desorbers for absorption heat pumps. As such, this review involved an exhaustive and detailed scrutiny of studies on pool desorbers, falling-film desorbers, and forced flow desorbers, detailing the experimenting techniques, test conditions, working fluids used, and the latest advances in desorber designs.

The literature review shows that the first studies were focused on characterizing, seeing, and understanding the pool boiling phenomenon. Interest then moved on from the boiling process to falling-film and forced flow configurations given the better flow hydrodynamics and the possibility of developing more compact desorbers. However, very few studies in falling-film and forced flow processes have included visual observation investigations.

Most of the studies reviewed have focused on the characterization of desorbers to identify the limiting parameters and the mechanisms responsible for the boiling at the conditions studied. In falling-film boiling, the wettability of the tube was found to be the main concern and object of study at different operating conditions, while few studies identified diffusion and nucleate boiling as the mechanisms responsible for boiling heat transfer. In the forced flow boiling process, the variation in mass flow and heat flow is of special interest if the predominant effects of diffusion, convective, and nucleate boiling are to be identified. In general, it was noted that convective boiling is predominant at high mass flows, whereas nucleate boiling is responsible for boiling heat transfer at low mass flows and high heat fluxes. In the case of diffusion, it was found to be responsible for boiling processes at low wall superheat temperatures and at low solution flows.

Comparing the number of studies reported on desorbers to those carried out on absorbers for absorption heat pumps [17], it is noteworthy that the number of investigations on desorbers is significantly lower. Moreover, this review provides evidence that the main technique employed for boiling enhancement and the design of more compact desorbers, is the use of advanced surfaces. The latest desorber design concepts involve the use of plates with extended surfaces as well as the use of membranes. Very few investigations available in the literature are related to the use of additives or nanofluids to improve heat and mass transfer in desorbers for absorption heat pumps. This means that studies involving surfactants or nanoparticles are still at an early stage of development. Therefore, the potential for research into the application of passive intensification techniques, such as the use of surfactants and nanofluids, is promising and likely to be in line with the advances and techniques employed in manufacturing absorbers.

Finally, there is a great need for more research to be carried out on the boiling process in advanced designs using conventional and promising working fluids including additives at the required operating conditions for different configurations of absorption heat pumps. Proposals for correlations that involve bubble hydrodynamics and their validation will also be the focus of new studies which may serve to contribute to the further development of absorption heat pump technologies.

Declaration of Competing Interest

None.

Acknowledgements

This study was also possible due to the support of the Universidad de la Costa and Minciencia through the Index Project CONV-15-2020.

References

[1] G.A. Florides, S.A. Tassou, S.A. Kalogirou, L.C. Wrobel, Review of solar and low energy cooling technologies for buildings, Renew. Sustain. Energy Rev. 6 (2002) 557–572.
[2] K.R. Ullah, R. Saidur, H.W. Ping, R.K. Akikur, N.H. Shuvo, A review of solar thermal refrigeration and cooling methods, Renew. Sustain. Energy Rev. 24 (2013) 499–513, doi:10.1016/J.RSER.2013.03.024.
[3] R. Best, I. Pilatowsky, Solar assisted cooling with sorption systems: status of the research in Mexico and Latin America, Int. J. Refrig. 21 (1998) 100–115, doi:10.1016/S0140-7007(97)00051-0.
[4] J. Mendoza, J. Rhenals, A. Avila, A. Martinez, T. De la Vega, E. Durango, Heat absorption cooling with renewable energies: a case study with photovoltaic solar energy and biogas in Cordoba, Colombia, INGE CUC 17 (2021) 1–10, doi:10.17981/ingecuc.17.2.2021.01.
[5] S. Yang, Y. Qian, Y. Wang, S. Yang, A novel cascade absorption heat transformer process using low grade waste heat and its application to coal to synthetic natural gas, Appl. Energy. 202 (2017) 42–52, doi:10.1016/j.apenergy.2017.04.028.
[6] C. Amaris, B.C. Miranda, M. Balbis-Morejón, Experimental thermal performance and modelling of a waste heat recovery unit in an energy cogeneration system, Therm. Sci. Eng. Prog. (2020) 20, doi:10.1016/j.tsep.2020.100684.
[7] M. Moya, J.C. Bruno, P. Eguia, E. Torres, I. Zamora, A. Coronas, Performance analysis of a trigeneration system based on a micro gas turbine and an air-cooled, indirect fired, ammonia-water absorption chiller, Appl. Energy. 88 (2011) 4424–4440, doi:10.1016/j.apenergy.2011.05.021.
[8] Y.T. Ge, S.A. Tassou, I. Chaer, N. Suguartha, Performance evaluation of a trigeneration system with simulation and experiment, Appl. Energy. 86 (2009) 2317–2326, doi:10.1016/j.apenergy.2009.03.018.
[9] D.S. Ayou, J.C. Bruno, R. Saravanan, A. Coronas, An overview of combined absorption power and cooling cycles, Renew. Sustain. Energy Rev. 21 (2013) 728–748, doi:10.1016/j.rser.2012.12.068.
[10] X. Wang, A. Bierwirth, A. Christ, P. Whittaker, K. Regenauer-Lieb, H.T. Chua, Application of geothermal absorption air-conditioning system: a case study, Appl. Therm. Eng., Pergamon. (2013) 71–80, doi:10.1016/j.applthermaleng.2012.05.011.
[11] P. Srikhirin, S. Aphornratana, S. Chungpaibulpatana, A review of absorption refrigeration technologies, Renew. Sustain. Energy Rev. 5 (2001) 343–372, doi:10.1016/S1364-0321(01)00003-X.
[12] C. Oronel, C. Amaris, M. Bourouis, M. Vallès, Heat and mass transfer in a bubble plate absorber with $NH_3/LiNO_3$ and $NH_3/(LiNO_3 + H_2O)$ mixtures, Int. J. Therm. Sci. 63 (2013), doi:10.1016/j.ijthermalsci.2012.07.007.
[13] C. Amaris, M.E. Alvarez, M. Vallès, M. Bourouis, Performance assessment of an $NH_3/LiNO_3$ bubble plate absorber applying a semi-empirical model and artificial neural networks, Energies 13 (2020), doi:10.3390/en13174313.
[14] C. Amaris, M. Bourouis, M. Vallès, Effect of advanced surfaces on the ammonia absorption process with $NH_3/LiNO_3$ in a tubular bubble absorber, Int. J. Heat Mass Transf. 72 (2014), doi:10.1016/j.ijheatmasstransfer.2014.01.031.
[15] C. Amaris, Intensification of NH_3 Bubble Absorption Process Using Advanced Surfaces and Carbon Nanotubes For $NH_3/LiNO_3$ Absorption Chillers, Universitat Rovira i Virgili, Tarragona, Spain, 2013 https://www.tdx.cat/handle/10803/128504.
[16] C. Amaris, M. Bourouis, M. Vallès, Passive intensification of the ammonia absorption process with $NH_3/LiNO_3$ using carbon nanotubes and advanced surfaces in a tubular bubble absorber, Energy 68 (2014) 519–528, doi:10.1016/j.energy.2014.02.039.
[17] C. Amaris, M. Vallès, M. Bourouis, Vapour absorption enhancement using passive techniques for absorption cooling/heating technologies: a review, Appl. Energy. 231 (2018) 826–853, doi:10.1016/j.apenergy.2018.09.071.
[18] R.L. Mohanty, M.K. Das, A critical review on bubble dynamics parameters influencing boiling heat transfer, Renew. Sustain. Energy Rev. 78 (2017) 466–494, doi:10.1016/j.rser.2017.04.092.
[19] M.R. Kærn, A. Modi, J.K. Jensen, J.G. Andreasen, F. Haglind, An assessment of in-tube flow boiling correlations for ammonia-water mixtures and their influence on heat exchanger size, Appl. Therm. Eng. 93 (2016) 623–638, doi:10.1016/j.applthermaleng.2015.09.106.
[20] P. Gupta, M. Hayat, R. Srivastava, A review on nucleate pool boiling heat transfer of binary mixtures, Asian J. Water, Environ. Pollut. 16 (2019) 27–34, doi:10.3233/AJW190016.
[21] J. Xu, Y. Wang, R. Yang, W. Liu, H. Wu, Y. Ding, Y. Li, A review of boiling heat transfer characteristics in binary mixtures, Int. J. Heat Mass Transf. 164 (2021), doi:10.1016/j.ijheatmasstransfer.2020.120570.
[22] D. Jung, H. Lee, D. Bae, S. Oho, Nucleate boiling heat transfer coefficients of flammable refrigerants, Int. J. Refrig. 27 (2004) 409–414, doi:10.1016/j.ijrefrig.2003.11.007.
[23] D. Jung, Y. Kim, Y. Ko, K. Song, Nucleate boiling heat transfer coefficients of pure halogenated refrigerants, Int. J. Refrig. 26 (2003) 240–248, doi:10.1016/S0140-7007(02)00040-3.
[24] M.G. Cooper, Saturation nucleate pool boiling - a simple correlation., Inst. Chem. Eng. Symp. Ser. (1984) 785–793, doi:10.1016/b978-0-85295-175-0.50013-8.
[25] I.L. Mostinski, Application of the rule of corresponding states for calculation of heat transfer and critical heat flux. 4, 66., Teploenergetika 4 (1963) 66.
[26] K. Stephan, M. Abdelsalam, Heat-transfer correlations for natural convection boiling, Int. J. Heat Mass Transf. 23 (1980) 73–87, doi:10.1016/0017-9310(80)90140-4.

[27] D. Gorenflo, D. Kenning, Pool Boiling, in: VDI Heat Atlas, 2nd ed., Springer, 2010, pp. 757–792, doi:10.1007/978-3-540-77877-6.

[28] S.G. Kandlikar, A general correlation for saturated two-phase flow boiling heat transfer inside horizontal and vertical tubes, J. Heat Transfer. 112 (1990) 219–228, doi:10.1115/1.2910348.

[29] G. Barthau, Active nucleation site density and pool boiling heat transfer-an experimental study, Int. J. Heat Mass Transf. 35 (1992) 271–278, doi:10.1016/0017-9310(92)90266-U.

[30] R.J. Benjamin, A.R. Balakrishnan, Nucleation Site Density in Pool Boiling of Saturated Pure Liquids: effect of Surface Microroughness and Surface and Liquid Physical Properties, Exp. Therm. Fluid Sci. 15 (1997) 32–42, doi:10.1016/S0894-1777(96)00168-9.

[31] R.J. Benjamin, A.R. Balakrishnan, Nucleate pool boiling heat transfer of pure liquids at low to moderate heat fluxes, Int. J. Heat Mass Transf. 39 (1996) 2495–2504, doi:10.1016/0017-9310(95)00320-7.

[32] G. Sateesh, S.K. Das, A.R. Balakrishnan, Analysis of pool boiling heat transfer: effect of bubbles sliding on the heating surface, Int. J. Heat Mass Transf. 48 (2005) 1543–1553, doi:10.1016/j.ijheatmasstransfer.2004.10.033.

[33] H. Chu, B. Yu, A new comprehensive model for nucleate pool boiling heat transfer of pure liquid at low to high heat fluxes including CHF, Int. J. Heat Mass Transf. 52 (2009) 4203–4210, doi:10.1016/j.ijheatmasstransfer.2009.04.010.

[34] C. Gerardi, J. Buongiorno, L.-.W. Hu, T. McKrell, Study of bubble growth in water pool boiling through synchronized, infrared thermometry and high-speed video, Int. J. Heat Mass Transf. 53 (2010) 4185–4192, doi:10.1016/j.ijheatmasstransfer.2010.05.041.

[35] B. Yu, P. Cheng, A fractal model for nucleate pool boiling heat transfer, J. Heat Transf. 124 (2002) 1117–1124, doi:10.1115/1.1513580.

[36] U. Wenzel, F. Balzer, M. Jamialahmadi, H. MÜller-Steinhagen, Pool boiling heat transfer coefficients for binary mixtures of acetone, isopropanol, and water, Heat Transf. Eng. 16 (1995) 36–43, doi:10.1080/01457639508939843.

[37] K.E. Gungor, R.H.S. Winterton, A general correlation for flow boiling in tubes and annuli, Int. J. Heat Mass Transf. 29 (1986) 351–358, doi:10.1016/0017-9310(86)90205-X.

[38] K.E. Gungor, R.H.S. Winterton, Simplified general correlation for saturated flow boiling and comparisons of correlations with data., Chem. Eng. Res. Des. 65 (1987) 148–156.

[39] S.G. Kandlikar, A model for correlating flow boiling heat transfer in augmented tubes and compact evaporators, J. Heat Transf. 113 (1991) 966–972, doi:10.1115/1.2911229.

[40] D.L. Bennett, J.C. Chen, Forced convective boiling in vertical tubes for saturated pure components and binary mixtures, AIChE J. 26 (1980) 454–461, doi:10.1002/aic.690260317.

[41] E.U. Schlunder, Heat transfer in nucleate boiling of mixtures, Int. Chem. Eng. 23 (1983) 589–599.

[42] J.R. Thome, S. Shakir, A new correlation for nucleate pool boiling of aqueous mixtures, AIChE Symp. Ser. (1987) 46–51.

[43] J.R. Thome, R.A.W. Shock, Boiling of Multicomponent Liquid Mixtures, Adv. Heat Transf. 16 (1984) 59–156, doi:10.1016/S0065-2717(08)70204-1.

[44] Y. Fujita, Q. Bai, Critical heat flux of binary mixtures in pool boiling and its correlation in terms of Marangoni number, Int. J. Refrig. 20 (1997) 616–622, doi:10.1016/S0140-7007(97)00026-1.

[45] G.V. Rao, A.R. Balakrishnan, Heat transfer in nucleate pool boiling of multicomponent mixtures, Exp. Therm. Fluid Sci. 29 (2004) 87–103, doi:10.1016/j.expthermflusci.2004.02.001.

[46] S.A. Alavi Fazel, M. Mahboobpour, Pool boiling heat transfer in monoethyleneglycol aqueous solutions, Exp. Therm. Fluid Sci. 48 (2013) 177–183, doi:10.1016/j.expthermflusci.2013.02.021.

[47] S.J.D. Van Stralen, The mechanism of nucleate boiling in pure liquids and in binary mixtures-part I, Int. J. Heat Mass Transf. 9 (1966), doi:10.1016/0017-9310(66)90025-1.

[48] W.F. Calus, P. Rice, Pool boiling-binary liquid mixtures, Chem. Eng. Sci. 27 (1972) 1687–1697, doi:10.1016/0009-2509(72)80083-6.

[49] W.F. Calus, D.J. Leonidopoulos, Pool boiling-Binary liquid mixtures, Int. J. Heat Mass Transf. 17 (1974) 249–256, doi:10.1016/0017-9310(74)90086-6.

[50] H. Jungnickel, P. Wassilew, W.E. Kraus, Investigations on the heat transfer of boiling binary refrigerant mixtures, Int. J. Refrig. 3 (1980) 129–133, doi:10.1016/0140-7007(80)90092-4.

[51] J.R. Thome, Prediction of binary mixture boiling heat transfer coefficients using only phase equilibrium data | Prevision du transfert thermique par ebullition d'un melange binaire, a partir des donnees d'equilibre de phase | Berechnung von Wärmeübergangskoeffiziente, Int. J. Heat Mass Transf. 26 (1983) 965–974, doi:10.1016/S0017-9310(83)80121-5.

[52] T. Inoue, N. Kawae, M. Monde, Characteristics of heat transfer coefficient during nucleate pool boiling of binary mixtures: improvement of correlation and its physical meaning, Heat Mass Transf. Und Stoffuebertragung. 33 (1998) 337–344, doi:10.1007/s002310050199.

[53] D. Steiner, J. Taborek, Flow boiling heat transfer in vertical tubes correlated by an asymptotic model, Heat Transf. Eng. 13 (1992) 43–69, doi:10.1080/01457639208939774.

[54] M.P. Mishra, H.K. Varma, C.P. Sharma, Heat Transfer Coefficients in Forced Convection Evaporation of Refrigerants Mixtures, Lett. Heat Mass Transf. 8 (1981) 127–136.

[55] M. Li, C. Dang, E. Hihara, Flow boiling heat transfer of HFO1234yf and HFC32 refrigerant mixtures in a smooth horizontal tube: part II. Prediction method, Int. J. Heat Mass Transf. 64 (2013) 591–608, doi:10.1016/j.ijheatmasstransfer.2013.04.047.

[56] I.L. Pioro, W. Rohsenow, S.S. Doerffer, Nucleate pool-boiling heat transfer. II: assessment of prediction methods, Int. J. Heat Mass Transf. 47 (2004) 5045–5057, doi:10.1016/j.ijheatmasstransfer.2004.06.020.

[57] B. Thonon, A. Feldman, L. Margat, C. Marvillet, Transition from nucleate boiling to convective boiling in compact heat exchangers, Int. J. Refrig. 20 (1997) 592–597, doi:10.1016/S0140-7007(97)00049-2.

[58] Y.T. Kang, Y. Kunugi, T. Kashiwagi, Review of advanced absorption cycles: performance improvement and temperature lift enhancement, Int. J. Refrig. 23 (2000) 388–401.

[59] W. Wu, B. Wang, W. Shi, X. Li, Absorption heating technologies: a review and perspective, Appl. Energy. 130 (2014), doi:10.1016/j.apenergy.2014.05.027.

[60] J. Sun, L. Fu, S. Zhang, A review of working fluids of absorption cycles, Renew. Sustain. Energy Rev. 16 (2012) 1899–1906, doi:10.1016/j.rser.2012.01.011.

[61] F. Táboas, Estudio Del Proceso De Ebullición Forzada De La Mezcla Amoniaco/Agua En Intercambiadores De Placas Para Equipos De Refrigeración Por Absorción, Universitat Rovira i Virgili, Tarragona, Spain, 2006 https://www.tesisenred.net/handle/10803/8491.

[62] W.W.S. Charters, V.R. Megler, W.D. Chen, Y.F. Wang, Atmospheric and subatmospheric boiling of H_2O and $LiBr/H_2O$ solutions, Int. J. Refrig. 5 (1982) 107–114, doi:10.1016/0140-7007(82)90085-8.

[63] H.K. Varma, R.K. Mehrotra, K.N. Agrawal, S. Singh, Heat transfer during pool boiling of LiBr-water solutions at subatmospheric pressures, Int. Commun. Heat Mass Transf. 21 (1994) 539–548, doi:10.1016/0735-1933(94)90053-1.

[64] T. Inoue, M. Monde, Y. Teruya, Pool boiling heat transfer in binary mixtures of ammonia/water, Int. J. Heat Mass Transf. 45 (2002) 4409–4415, doi:10.1016/S0017-9310(02)00153-9.

[65] H. Arima, M. Monde, Y. Mitsutake, Heat transfer in pool boiling of ammonia/water mixture, Heat Mass Transf. Und Stoffuebertragung. 39 (2003) 535–543, doi:10.1007/s00231-002-0302-2.

[66] F. Táboas, M. Vallès, M. Bourouis, A. Coronas, Pool boiling of ammonia/water and its pure components: comparison of experimental data in the literature with the predictions of standard correlations, Int. J. Refrig. 30 (2007) 778–788, doi:10.1016/j.ijrefrig.2006.12.009.

[67] T. Inoue, M. Monde, Prediction of pool boiling heat transfer coefficient in ammonia/water mixtures, Heat Transf. - Asian Res. 38 (2009) 65–72, doi:10.1002/htj.20234.

[68] A. Sathyabhama, T.P. Ashok Babu, Nucleate pool boiling heat transfer measurement and flow visualization for ammonia-water mixture, J. Heat Transf. 133 (2011), doi:10.1115/1.4004258.

[69] A. Sathyabhama, T.P. Ashok Babu, Experimental investigation in pool boiling heat transfer of ammonia/water mixture and heat transfer correlations, Int. J. Heat Fluid Flow. 32 (2011) 719–729, doi:10.1016/j.ijheatfluidflow.2011.02.007.

[70] T. Inoue, Y. Teruya, M. Monde, Enhancement of pool boiling heat transfer in water and ethanol/water mixtures with surface-active agent, Int. J. Heat Mass Transf. 47 (2004) 5555–5563, doi:10.1016/j.ijheatmasstransfer.2004.05.037.

[71] W.F. Calus, P. Rice, Pool boiling-binary mixtures, Chem. Eng. Sci. 27 (1972) 1687–1697.

[72] K. Stephan, M. Korner, Calculation of heat transfer in evaporating binary liquid mixtures, Chem.-Ing. Tech. 41 (1969) 409–417.

[73] A. Sathyabhama, T.P. Ashok Babu, Experimental study of nucleate pool boiling heat transfer to ammonia-water-lithium bromide solution, Exp. Therm. Fluid Sci. 35 (2011) 1046–1054, doi:10.1016/j.expthermflusci.2011.02.007.

[74] T. Inoue, M. Monde, Enhancement of nucleate pool boiling heat transfer in ammonia/water mixtures with a surface-active agent, Int. J. Heat Mass Transf. 55 (2012) 3395–3399, doi:10.1016/j.ijheatmasstransfer.2012.03.004.

[75] A. Sathyabhama, T.P. Ashok Babu, Experimental investigation of pool boiling heat transfer in ammonia-water-lithium nitrate solution, Exp. Heat Transf. 25 (2012) 127–138, doi:10.1080/08916152.2011.582568.

[76] J.-.Y. Jung, E.S. Kim, Y. Nam, Y.T. Kang, The study on the critical heat flux and pool boiling heat transfer coefficient of binary nanofluids (H_2O/LiBr + Al_2O_3), Int. J. Refrig. 36 (2013) 1056–1061, doi:10.1016/j.ijrefrig.2012.11.021.

[77] X.-.D. Han, S.-.W. Zhang, Y. Tang, W. Yuan, B. Li, Mass transfer enhancement for LiBr solution using ultrasonic wave, J. Cent. South Univ. 23 (2016) 405–412, doi:10.1007/s11771-016-3085-1.

[78] T. Inoue, M. Monde, Enhancement of nucleate pool boiling heat transfer in ammonia/water mixtures with a surface-active agent, Int. J. Heat Mass Transf. 55 (2012) 3395–3399, doi:10.1016/j.ijheatmasstransfer.2012.03.004.

[79] D. Kim, M. Kim, Heat transfer enhancement characteristics for falling-film evaporation on horizontal enhanced tubes with aqueous LiBr solution, J. Enhanc. Heat Transf. 6 (1999) 61–69, doi:10.1615/JEnhHeatTransf.v6.i1.60.

[80] K. Tuzla, K. Warn, J.C. Chen, Boiling inception in falling films of binary mixtures, Exp. Heat Transf. 8 (1995) 177–184, doi:10.1080/08916159508946499.

[81] C. Shi, C. Xu, H. Hu, Y. Ying, Study on falling film generation heat transfer of lithium bromide solution in vertical tubes, J. Therm. Sci. 18 (2009) 241–245, doi:10.1007/s11630-009-0241-z.

[82] C. Shi, Q. Chen, T.-.C. Jen, W. Yang, Heat transfer performance of lithium bromide solution in falling film generator, Int. J. Heat Mass Transf. 53 (2010) 3372–3376, doi:10.1016/j.ijheatmasstransfer.2010.02.051.

[83] M.D. Determan, S. Garimella, Ammonia-water desorption heat and mass transfer in microchannel devices, Int. J. Refrig. 34 (2011) 1197–1208, doi:10.1016/j.ijrefrig.2011.02.004.

[84] Y. Lazcano-Véliz, J. Siqueiros, D. Juárez-Romero, L.I. Morales, J. Torres-Merino, Analysis of effective wetting area of a horizontal generator for an absorption heat transformer, Appl. Therm. Eng. 62 (2014) 845–849, doi:10.1016/j.applthermaleng.2013.09.043.
[85] C.M. Keinath, D. Hoysall, J.C. Delahanty, M.D. Determan, S. Garimella, Experimental assessment of a compact branched tray generator for ammonia-water desorption, Sci. Technol. Built Environ. 21 (2015) 348–356, doi:10.1080/23744731.2014.1000797.
[86] J.C. Delahanty, S. Garimella, M.A. Garrabrant, Design of compact microscale geometries for ammonia-water desorption, Sci. Technol. Built Environ. 21 (2015) 365–374, doi:10.1080/23744731.2015.1015906.
[87] M. Olbricht, J. Addy, A. Luke, Heat and Mass Transfer in a Falling Film Evaporator with Aqueous Lithium Bromide Solution, J. Phys. Conf. Ser. 745 (2016) 032056.
[88] M. Mortazavi, M. Schmid, S. Moghaddam, Compact and efficient generator for low grade solar and waste heat driven absorption systems, Appl. Energy. 198 (2017) 173–179, doi:10.1016/j.apenergy.2017.04.054.
[89] R. Nasr Isfahani, K. Sampath, S. Moghaddam, Nanofibrous membrane-based absorption refrigeration system, Int. J. Refrig. (2013), doi:10.1016/j.ijrefrig.2013.07.019.
[90] Y. Lazcano-Véliz, J.A. Hernández, D. Juárez-Romero, A. Huicochea-Rodríguez, A. Álvarez-Gallegos, J. Siqueiros, Improved of effective wetting area and film thickness on a concentric helical bank of a generator for an absorption heat transformer, Appl. Therm. Eng. 106 (2016) 1319–1328, doi:10.1016/j.applthermaleng.2016.06.127.
[91] Y. Lazcano-Véliz, J.A. Hernández, D. Juárez-Romero, M. Bourouis, A. Coronas, J. Siqueiros, Energy efficiency assessment in the generator of an absorption heat transformer from measurement falling film thickness on helical coils, Appl. Energy. 208 (2017) 1274–1284, doi:10.1016/j.apenergy.2017.09.026.
[92] T. Hu, X. Xie, Y. Jiang, Design and experimental study of a plate-type falling-film generator for a LiBr/H_2O absorption heat pump | Conception et étude expérimentale d'un générateur à film tombant de type plaque pour une pompe à chaleur à absorption au LiBR/H_2, Int. J. Refrig. 74 (2017) 302–310, doi:10.1016/j.ijrefrig.2016.09.024.
[93] M.A. Staedter, S. Garimella, Design and modeling of a microscale diabatic distillation column for small capacity ammonia-water absorption systems, Int. J. Refrig. 94 (2018) 161–173, doi:10.1016/j.ijrefrig.2018.06.018.
[94] M.A. Staedter, S. Garimella, Heat and mass transfer in microscale diabatic distillation columns for ammonia-water desorption and rectification | Transfert de chaleur et de masse dans les colonnes de distillation diabatique pour la désorption et la rectification du mélange ammoniac-ea, Int. J. Refrig. 95 (2018) 10–20, doi:10.1016/j.ijrefrig.2018.07.034.
[95] M.A. Staedter, S. Garimella, Direct-coupled desorption for small capacity ammonia-water absorption systems, Int. J. Heat Mass Transf. 127 (2018) 196–205, doi:10.1016/j.ijheatmasstransfer.2018.06.118.
[96] C.M. Keinath, A. Krishna Nagavarapu, J.C. Delahanty, S. Garimella, M.A. Garrabrant, Experimental assessment of alternative compact configurations for ammonia-water desorption, Appl. Therm. Eng. (2019) 161, doi:10.1016/j.applthermaleng.2019.113852.
[97] J.A. Hernández-Magallanes, W. Rivera, Boiling heat transfer coefficients in a falling film helical coil heat exchanger for the NH3-LiNO3 mixture, J. Heat Transfer. (2019) 141, doi:10.1115/1.4043300.
[98] J.C. Delahanty, M. Hughes, S. Garimella, Desorber and rectifier geometries for ammonia-water absorption systems; part I: experimental approach and heat transfer, Int. J. Refrig. (2020), doi:10.1016/j.ijrefrig.2020.10.020.
[99] T. Hu, X. Xie, Y. Jiang, A detachable plate falling film generator and condenser coupling using lithium bromide and water as working fluids | Générateur de film tombant à plaque détachable raccordé à un condenseur utilisant du bromure de lithium et de l'eau comme fluides actifs, Int. J. Refrig. 98 (2019) 120–128, doi:10.1016/j.ijrefrig.2018.10.007.
[100] J. Jurng, C. Woo Park, On the performance of a desorber for absorption heat pumps with a thermosyphon and a surfaceflame burner, Appl. Therm. Eng. 18 (1998) 83.
[101] W. Rivera, R. Best, Boiling heat transfer coefficients inside a vertical smooth tube for water/ammonia and ammonia/lithium nitrate mixtures, Int. J. Heat Mass Transf. 42 (1999) 905–921, doi:10.1016/S0017-9310(98)00211-7.
[102] S.B. Riffat, S. Wu, B. Bol, Pervaporation membrane process for vapour absorption system, Int. J. Refrig. 27 (2004) 604–611, doi:10.1016/j.ijrefrig.2004.03.005.
[103] T. Khir, A. Ben Brahim, R.K. Jassim, Boiling for convection force of mixing water-ammonia in a vertical tube | Ébullition par convection forcée des mélanges eau-ammoniac dans un tube vertical, Can. J. Chem. Eng. 83 (2005) 466–476, doi:10.1002/cjce.5450830309.
[104] T. Khir, R.K. Jassim, N. Ghaffour, A.B. Brahim, Experimental study on forced convective boiling of ammonia-water mixtures in a vertical smooth tube, Arab, J. Sci. Eng. 30 (2005) 47–64.
[105] J.D. Thorud, J. Liburdy, D. Pence, Microchannel membrane separation applied to confined thin film desorption, Exp. Therm. Fluid Sci. 30 (2006) 713–723.
[106] J.D. Marcos, M. Izquierdo, R. Lizarte, E. Palacios, C.A. Infante Ferreira, Experimental boiling heat transfer coefficients in the high temperature generator of a double effect absorption machine for the lithium bromide/water mixture, Int. J. Refrig. 32 (2009) 627–637, doi:10.1016/j.ijrefrig.2009.02.003.
[107] B. Thonon, Design method for plate evaporators and condensers, 1st Int. Conf. Process Intensif. Chem. Ind 18 (1995) 37–47.
[108] G. Hewitt, G.L. Shires, T.R. Bott, Process Heat Transfer, Begell House, 1994.
[109] Z. Wang, Z. Gu, S. Feng, Y. Li, Application of vacuum membrane distillation to lithium bromide absorption refrigeration system, Int. J. Refrig. 32 (2009) 1587–1596, doi:10.1016/j.ijrefrig.2009.07.002.
[110] F. Táboas, M. Vallès, M. Bourouis, A. Coronas, Flow boiling heat transfer of ammonia/water mixture in a plate heat exchanger, Int. J. Refrig. 33 (2010) 695–705, doi:10.1016/j.ijrefrig.2009.12.005.
[111] A. Zacarías, R. Ventas, M. Venegas, A. Lecuona, Boiling heat transfer and pressure drop of ammonia-lithium nitrate solution in a plate generator, Int. J. Heat Mass Transf. 53 (2010) 4768–4779, doi:10.1016/j.ijheatmasstransfer.2010.06.015.
[112] P. Balamurugan, A. Mani, Experimental studies on heat and mass transfer in tubular generator for R134a-DMF absorption refrigeration system, Int. J. Therm. Sci. 61 (2012) 118–128, doi:10.1016/j.ijthermalsci.2012.06.001.
[113] P. Balamurugan, A. Mani, Heat and mass transfer studies on compact generator of R134a/DMF vapour absorption refrigeration system, Int. J. Refrig. 35 (2012) 506–517, doi:10.1016/j.ijrefrig.2012.01.009.
[114] P. Balamurugan, A. Mani, Comparison of compact and tubular generators performance for R134a-DMF, Exp. Therm. Fluid Sci. 45 (2013) 54–62, doi:10.1016/j.expthermflusci.2012.10.007.
[115] M. Venegas, A. Zacarías, C. Vereda, A. Lecuona, R. Ventas, Subcooled and saturated boiling of ammonia-lithium nitrate solution in a plate-type generator for absorption machines, Int. J. Heat Mass Transf. 55 (2012) 4914–4922, doi:10.1016/j.ijheatmasstransfer.2012.04.061.
[116] F. Táboas, M. Vallès, M. Bourouis, A. Coronas, Assessment of boiling heat transfer and pressure drop correlations of ammonia/water mixture in a plate heat exchanger, Int. J. Refrig. 35 (2012) 633–644, doi:10.1016/j.ijrefrig.2011.10.003.
[117] D.-.H. Han, K.-.J. Lee, Y.-.H. Kim, Experiments on the characteristics of evaporation of R410A in brazed plate heat exchangers with different geometric configurations, Appl. Therm. Eng. 23 (2003) 1209–1225, doi:10.1016/S1359-4311(03)00061-9.
[118] V.D. Donowski, S.G. Kandlikar, Correlating evaporation heat transfer coefficient of refrigerant R134a in a plate heat exchanger, Eng. Found. Conf. Pool Flow Boil. (2000).
[119] R. Nasr Isfahani, A. Fazeli, S. Bigham, S. Moghaddam, Physics of lithium bromide (LiBr) solution dewatering through vapor venting membranes, Int. J. Multiph. Flow. 58 (2014) 27–38, doi:10.1016/j.ijmultiphaseflow.2013.08.005.
[120] S. Bigham, R. Nasr Isfahani, S. Moghaddam, Direct molecular diffusion and micro-mixing for rapid dewatering of LiBr solution, Appl. Therm. Eng. 64 (2014) 371–375, doi:10.1016/j.applthermaleng.2013.12.031.
[121] C. Amaris, M. Bourouis, M. Vallès, D. Salavera, A. Coronas, Thermophysical properties and heat and mass transfer of new working fluids in plate heat exchangers for absorption refrigeration systems, Heat Transf. Eng. 36 (2015) 388–395, doi:10.1080/01457632.2014.923983.
[122] F. Táboas, M. Bourouis, M. Valles, Boiling heat transfer and pressure drop of NH_3/$LiNO_3$ and NH_3/($LiNO_3$+H_2O) in a plate heat exchanger, Int. J. Therm. Sci. 105 (2016) 182–194, doi:10.1016/j.ijthermalsci.2016.02.003.
[123] C. Oronel, C. Amaris, M. Vallès, M. Bourouis, Experiments on the characteristics of saturated boiling heat transfer in a plate heat exchanger for ammonia/lithium nitrate and ammonia/(lithium nitratewater), in: 2010 3rd Int, Conf. Therm. Issues Emerg. Technol. Theory Appl. - Proceedings (2010) 217–225 ThETA3 2010, doi:10.1109/THETA.2010.5766401.
[124] J. Jiang, G. He, Y. Liu, Y. Liu, D. Cai, Flow boiling heat transfer characteristics and pressure drop of ammonia-lithium nitrate solution in a smooth horizontal tube, Int. J. Heat Mass Transf. 108 (2017) 220–231, doi:10.1016/j.ijheatmasstransfer.2016.12.004.
[125] J. Jiang, Y. Liu, G. He, Y. Liu, D. Cai, X. Liang, Experimental investigations and an updated correlation of flow boiling heat transfer coefficients for ammonia/lithium nitrate mixture in horizontal tubes, Int. J. Heat Mass Transf. 112 (2017) 224–235, doi:10.1016/j.ijheatmasstransfer.2017.04.135.
[126] J. Ibarra-Bahena, U. Dehesa-Carrasco, R.J. Romero, B. Rivas-Herrera, W. Rivera, Experimental assessment of a hydrophobic membrane-based desorber/condenser with H_2O/LiBr mixture for absorption systems, Exp. Therm. Fluid Sci. 88 (2017) 145–159, doi:10.1016/j.expthermflusci.2017.05.024.
[127] S.J. Hong, E. Hihara, C. Dang, Analysis of adiabatic heat and mass transfer of microporous hydrophobic hollow fiber membrane-based generator in vapor absorption refrigeration system, J. Memb. Sci. 564 (2018) 415–427, doi:10.1016/j.memsci.2018.07.048.
[128] D. Cai, Y. Liu, X. Liang, J. Jiang, M. Fan, G. He, Experimental investigation of flow boiling heat transfer characteristics in smooth horizontal tubes using NH_3/NaSCN solution as working fluid, Int. J. Heat Mass Transf. 127 (2018) 799–812, doi:10.1016/j.ijheatmasstransfer.2018.08.078.
[129] M. Venegas, N. García-Hernando, M. de Vega, Experimental evaluation of a membrane-based microchannel desorber operating at low desorption temperatures, Appl. Therm. Eng. 167 (2020), doi:10.1016/j.applthermaleng.2019.114781.
[130] J. Ibarra-Bahena, E. Venegas-Reyes, Y.R. Galindo-Luna, W. Rivera, R.J. Romero, A. Rodríguez-Martínez, U. Dehesa-Carrasco, Feasibility analysis of a membrane desorber powered by thermal solar energy for absorption cooling systems, Appl. Sci. 10 (2020), doi:10.3390/app10031110.
[131] K. Li, G. He, J. Jiang, Y. Li, D. Cai, Flow boiling heat transfer characteristics and pressure drop of R290/oil solution in smooth horizontal tubes, Int. J. Heat Mass Transf. 119 (2018) 777–790, doi:10.1016/j.ijheatmasstransfer.2017.11.134.

[132] S. Zhou, X. Zhao, D. Cai, J. Deng, Y. Gao, G. He, Experimental evaluation on flow boiling heat transfer of R290/POE-oil working fluid for absorption refrigeration in smooth horizontal tubes, Int. J. Therm. Sci. 159 (2021), doi:10.1016/j.ijthermalsci.2020.106641.
[133] L. Cheng, L. Liu, Boiling and two-phase flow phenomena of refrigerant-based nanofluids: fundamentals, applications and challenges, Int. J. Refrig., Elsevier (2013) 421–446, doi:10.1016/j.ijrefrig.2012.11.010.
[134] Y. Fujita, M. Tsutsui, Heat transfer in nucleate boiling of binary mixtures (Development of a heat transfer correlation), JSME Int. Journal, Ser. B Fluids Therm. Eng. 40 (1997) 134–141, doi:10.1299/jsmeb.40.134.
[135] T. Inoue, S. Kawae, M. Monde, Characteristics of heat transfer during nucleate pool boiling of binary mixtures, Trans. JSME. (1997) 1312–1319.